



Calhoun: The NPS Institutional Archive DSpace Repository

Theses and Dissertations

1. Thesis and Dissertation Collection, all items

1970

Finite element study of acoustic waves

Dean, Dennis Vale

Monterey, California; Naval Postgraduate School

<http://hdl.handle.net/10945/15009>

This publication is a work of the U.S. Government as defined in Title 17, United States Code, Section 101. Copyright protection is not available for this work in the United States.

Downloaded from NPS Archive: Calhoun



<http://www.nps.edu/library>

Calhoun is the Naval Postgraduate School's public access digital repository for research materials and institutional publications created by the NPS community.

Calhoun is named for Professor of Mathematics Guy K. Calhoun, NPS's first appointed -- and published -- scholarly author.

Dudley Knox Library / Naval Postgraduate School
411 Dyer Road / 1 University Circle
Monterey, California USA 93943

FINITE ELEMENT STUDY OF ACOUSTIC WAVES

by

Dennis Vale Dean

United States
Naval Postgraduate School



THEESIS

FINITE ELEMENT STUDY OF ACOUSTIC WAVES

by

Dennis Vale Dean

December 1970

This document has been approved for public release and sale; its distribution is unlimited.

T137598



Finite Element Study of Acoustic Waves

by

Dennis Vale Dean
Lieutenant Commander, United States Navy
B.S., United States Merchant Marine Academy, 1959

Submitted in partial fulfillment of the
requirements for the degree of

MASTER OF SCIENCE IN MECHANICAL ENGINEERING

from the
NAVAL POSTGRADUATE SCHOOL
December 1970

Theses D 182.8
c 1

ABSTRACT

The generation and propagation of small amplitude acoustic waves in a homogeneous, loss-free, compressible fluid is studied by the finite element method. A diaphragm mounted in an infinite rigid baffle generates acoustic waves in a semi-infinite fluid region. Steady-state pressure distribution is found for a hemispherical region with boundary reflection suppressed through use of a radiation condition. The computer program developed for the purpose utilizes iso-parametric finite elements with curvilinear boundaries. Incorporated in the program is a versatile mesh generator which minimizes the quantity of input data. Acceptable agreement with analytic results is obtained when there are at least four elements per wave-length.

TABLE OF CONTENTS

I.	INTRODUCTION -----	5
III.	FINITE ELEMENT FORMULATION OF THE GOVERNING EQUATION -----	8
A.	EQUATION OF MOTION -----	8
B.	SYSTEM OF ORDINARY DIFFERENTIAL EQUATIONS -----	8
C.	DIAPHRAGM BOUNDARY CONDITION -----	10
D.	RADIATION (NON-REFLECTION) BOUNDARY CONDITION -----	10
III.	GEOMETRY OF THE REGION -----	12
IV.	WAVE THEORY AT RADIATION BOUNDARIES -----	14
V.	COMPUTER SOLUTION TECHNIQUE -----	16
VI.	RESULTS -----	18
VII.	CONCLUSIONS -----	25
	APPENDIX A: COMPUTER OUTPUT -----	26
	APPENDIX B: COMPUTER PROGRAM -----	43
	APPENDIX C: ISO-PARAMETRIC ELEMENTS -----	61
	APPENDIX D: FINITE ELEMENT MESH GENERATOR -----	64
	APPENDIX E: MATRIX ELEMENT FORMULAS -----	67
	LIST OF REFERENCES -----	68
	INITIAL DISTRIBUTION LIST -----	69
	FORM DD 1473 -----	70

ACKNOWLEDGEMENTS

The author desires to express his appreciation to his thesis advisor, Dr. Robert E. Newton, Professor of Mechanical Engineering, U.S. Naval Postgraduate School, for conscientiously and attentively supervising the work throughout the development of this paper.

Personnel in the W. R. Church Computer Center, U.S. Naval Postgraduate School, greatly assisted in providing technical advice, facilities, and expedient service.

I. INTRODUCTION

The field of acoustics plays an important role in the development of the complex sonar systems used in the United States Navy today. It is the intent of this paper to open a new avenue to the study of the active sonar system. Attention is confined to the transducer and the periodic pressure field induced in a fluid medium by harmonic oscillations of the transducer piston or diaphragm.

The study is restricted to the steady-state performance of a transducer mounted in an infinite rigid baffle and radiating into a half-space filled with a homogeneous fluid. Both the pressure field and the acoustic impedance of the transducer are determined. Figure 1 illustrates the geometry of the region.

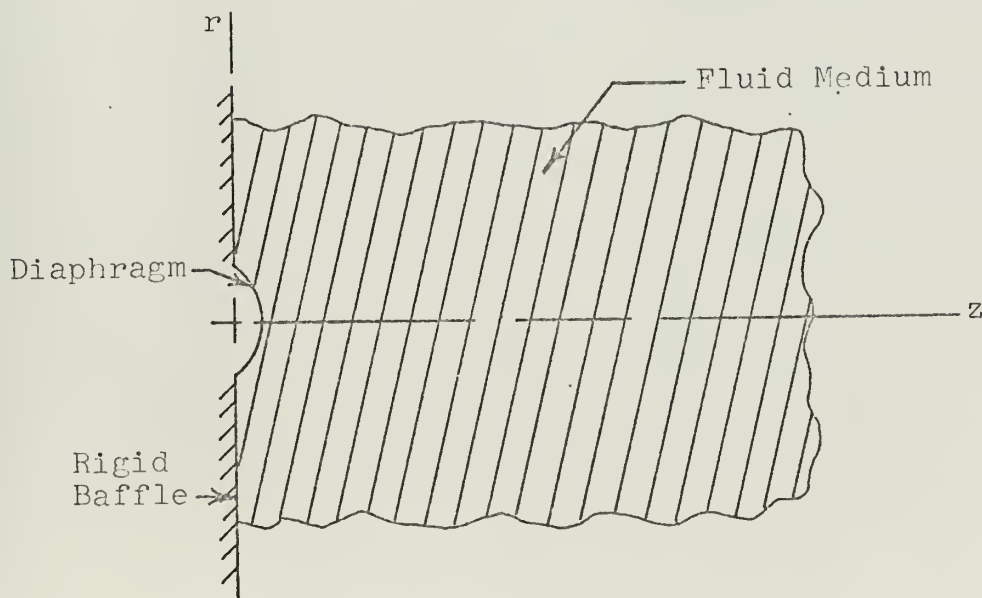


Figure 1. Geometry of Region.

The method used in this study is the two-dimensional finite element technique. Since it is manifestly impossible to represent an infinite region with a finite number of finite elements, the stratagem of the anechoic chamber is simulated mathematically. This is accomplished by using radiation (non-reflection) boundary conditions.

The diaphragm, being circular, forms a surface of revolution when deflected. Thus, the instantaneous pressure distribution has rotational symmetry about an axis through the diaphragm center and normal to the rigid baffle (z axis of Figure 1). A finite element assembly representing the region of interest may be constructed by dividing the corresponding portion of the $r-z$ plane of Figure 1 into sub-areas as shown in Figure 2.

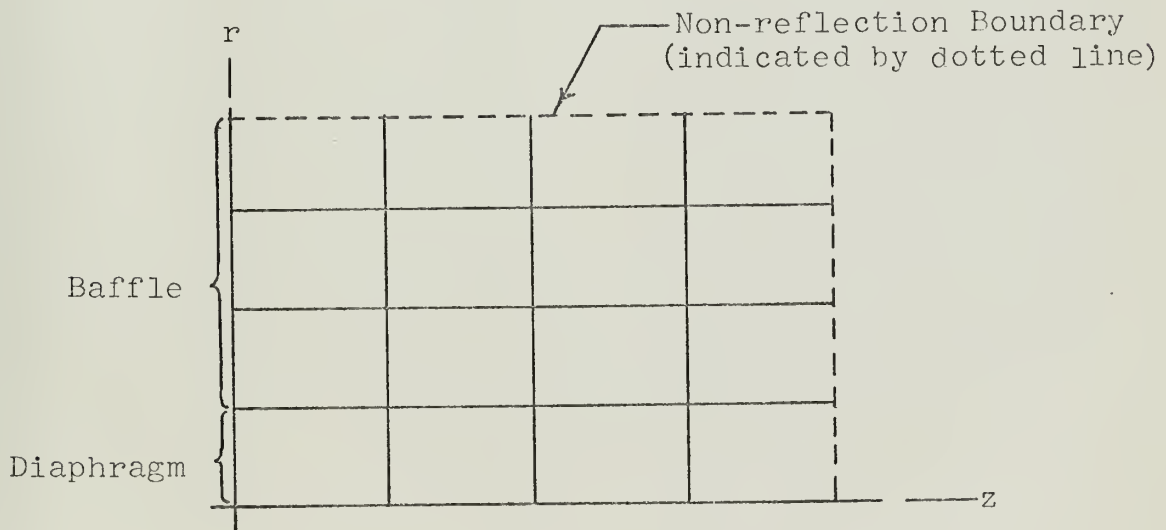


Figure 2. Finite Element Grid

In Figure 2, an individual rectangular element represents the cross-section of a toroidal element generated by revolution about the z axis. The rotational symmetry permits calculation of element properties using two-dimensional technique by simply taking the thickness (normal to the plane of the figure) proportional to r .

III. FINITE ELEMENT FORMULATION OF THE GOVERNING EQUATION

A. EQUATION OF FLUID MOTION

The governing partial differential equation for the pressure p in a homogeneous, inviscid, compressible fluid as used in acoustics (e.g., see Ref. [1]^{*}) is

$$\nabla^2 p = \frac{1}{c^2} \ddot{p} \quad (1)$$

where ∇^2 is the Laplacian operator, c is the acoustic velocity, and superior dots represent differentiation with respect to time. For the purpose of the present study, boundary conditions take the form

$$\frac{\partial p}{\partial n} = -\rho v_n \quad (2)$$

where the coordinate n is measured along the normal to the boundary surface, ρ is the fluid density, and v_n is the component of fluid particle velocity in the n direction.

B. SYSTEM OF ORDINARY DIFFERENTIAL EQUATIONS

The finite element method replaces Eqs. (1) and (2) by a set of simultaneous ordinary differential equations with independent variable time and dependent variables consisting of pressures at a large number of discrete points (nodes) of the region. The region is divided into a number of

*Numbers in brackets designate references listed on page 68.

sub-regions called "elements." Within each element it is postulated that the pressure p may be expressed in terms of the pressure p_i at the n nodes of the element. This relation is expressed as

$$p = \sum_{i=1}^n N_i p_i \quad (3)$$

where the "shape" (or interpolation) functions N_i are functions of the spatial coordinates. If the nodes are located at suitably chosen points on the element surface, unique sets of shape functions will guarantee the necessary continuity of pressure p along interelement boundaries as pointed out by Zienkiewicz [2]. The elements used in this study are two-dimensional eight-noded iso-parametric elements. Further details are given in Appendix C.

It has been shown by Zienkiewicz and Newton [3] that the finite element equation for k nodes, m of which are located on the fluid-diaphragm interface, may be written as

$$[Q]\{\ddot{p}\} + [D]\{\dot{p}\} + [H]\{p\} = -\rho[L]^T\{\ddot{\delta}\} \quad (4)$$

where $\{p\}$ is a $k \times 1$ vector of nodal pressures, $[Q]$, $[D]$, and $[H]$ are $k \times k$ symmetric matrices, $\{\delta\}$ is an $m \times 1$ vector of diaphragm displacements, and $[L]^T$ is a $k \times m$ matrix. Elements of $[Q]$, $[D]$, $[H]$, and $[L]^T$ are all real constants. Formulas for calculating these matrices are given in Appendix E. The terms $[D]\{\dot{p}\}$ and $[L]^T\{\ddot{\delta}\}$ represent boundary conditions and will be discussed in following sections.

C. DIAPHRAGM BOUNDARY CONDITION

The diaphragm displacement δ is a prescribed function of time. It can be represented by choosing a number of points (nodes) on the diaphragm and using a set of shape functions N_j' to interpolate the local displacement as

$$\delta = \sum_{j=1}^m N_j' \delta_j \quad (5)$$

where the δ_j are the displacements at the m diaphragm nodes.

The boundary condition of Eq. (2) is formulated in terms of the normal component v_n of fluid particle velocity. At the diaphragm surface this must, in the absence of cavitation, be equal to $\dot{\delta}$. Using this equality, the fluid-diaphragm interface condition gives the term

$$-\rho [L]^T \{ \ddot{\delta} \}$$

in the finite element equation (Eq. (4)). The resulting vector has nonzero elements only for those pressure nodes located on the diaphragm surface. It is noted that the boundary condition on the rigid baffle is a special case, in that the particle velocity $v_n = 0$, which implies $\dot{v}_n = 0$.

D. RADIATION (NON-REFLECTION) BOUNDARY CONDITION

A normally incident wave meeting the interface between two media will not be reflected if the specific acoustic impedances of the two media are equal. The specific acoustic impedance z is defined to be the ratio of pressure to

particle velocity. For plane harmonic waves this is a real quantity and the pressure can be given as

$$p = \rho c v_n \quad (6)$$

for a wave progressing in the positive n direction. Differentiating Eq. (6) with respect to time and using this result to eliminate \dot{v}_n from the boundary condition (Eq. (2)) gives

$$\frac{\partial p}{\partial n} = -\frac{1}{c} \dot{p} \quad (7)$$

Equation (7) then becomes the boundary condition for non-reflection of normally incident plane waves. The term

$$[D]\{p\}$$

in Eq. (4) results from this criterion. This vector has nonzero elements only for those nodes which lie on the non-reflecting portion of the boundary.

III. GEOMETRY OF THE REGION

The initial solution of the problem using the geometric configuration of Figure 2 resulted in significant error in the pressure distribution when the solution was checked against known results. The principal cause of this error was believed to be the shape of the non-reflection boundary. By the nature of the geometry, the harmonic oscillating diaphragm will create progressive pressure waves which propagate outward and strike the boundary of Figure 2 at various angles of incidence. The particle velocity, v_n , will not always be normal to the non-reflection boundary and the boundary condition required by Eq. (2) will not be satisfied. Thus, a modification to the representation of the boundary to provide substantially normal incidence led to the geometry illustrated in Figure 3. For this modified radiation boundary, in three dimensions the surface is hemispherical.

In order to represent adequately the circular arc of the non-reflection boundary, two-dimensional iso-parametric finite elements are used. The element thickness normal to the plane of the figure is directly proportional to the radius r . Iso-parametric elements are further discussed in Appendix C.

Note the distortion of the grid in Figure 3. The reason for this distortion and the method of generating the grid

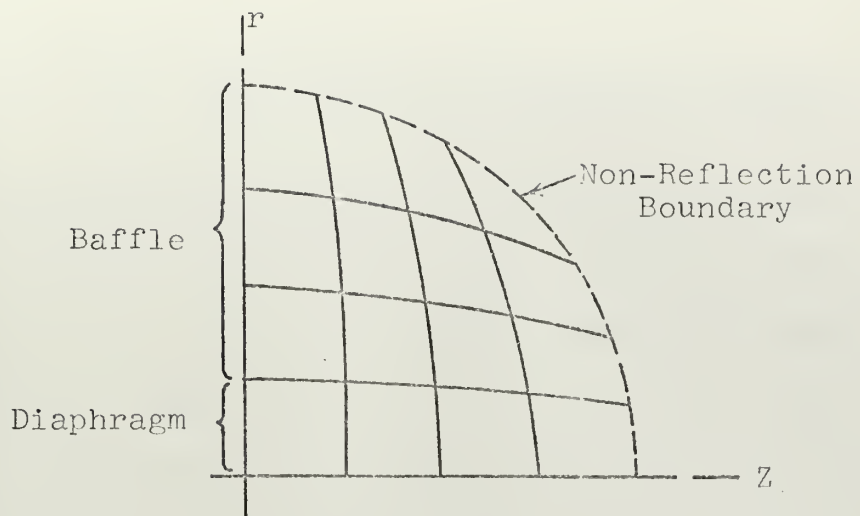


Figure 3. Modified Finite Element Region

pattern is discussed in Appendix D. The distorted "rectangles" still represent the cross sections of toroidal elements.

IV. WAVE THEORY AT RADIATION BOUNDARY

A one-dimensional study of a pulsating sphere acting on a fluid medium resulted in a more accurate solution when spherical wave theory at the non-reflection boundary was introduced. Based upon the success of these results, a further modification was made to the computer program (Appendix B) to incorporate spherical wave theory in the two-dimensional study. This was accomplished by developing the non-reflection boundary condition for spherically diverging waves as shown below.

The specific acoustic impedance for spherically diverging waves is given in Ref. [1] as

$$Z = \frac{p}{v_n} = \rho c \frac{\frac{\omega}{c} r}{\frac{\omega}{c} r - j} \quad (8)$$

where ω is the circular frequency and r is the radial distance from the "center." The particle acceleration \dot{v}_n can be written as

$$\dot{v}_n = j\omega v_n \quad (9)$$

which allows the boundary condition to be represented by

$$\frac{\partial p}{\partial r} = -\rho j\omega v_n \quad (10)$$

From Eqs. (8) and (10), the boundary condition is

$$\frac{\partial p}{\partial r} = - \frac{j\omega p}{c} \left[\frac{\frac{\omega}{c}r - j}{\frac{\omega}{c}r} \right] \quad (11)$$

or

$$\frac{\partial p}{\partial r} = - p \left(\frac{1}{r} + j \frac{\omega}{c} \right) \quad (12)$$

The imaginary term on the right hand side of Eq. (12) is represented by the term $[D]\{\dot{p}\} = j\omega[D]\{p\}$ in Eq. (4). Thus, the contribution of the real term can be written as

$$\frac{c}{r}[D]\{p\} \quad (13)$$

and can be added to the system of equations given in Eq. (4).

The spherical contribution is only added to the nodes which lie on the non-reflection boundary, thus providing a spherical wave approximation to the plane wave theory at the non-reflection boundary.

V. COMPUTER SOLUTION TECHNIQUE

Assume the diaphragm is oscillating with a harmonic displacement represented in the complex form by

$$\{\delta\} = \{\delta_0\} e^{j\omega t} \quad (14)$$

where $\{\delta_0\}$ is a vector of prescribed displacement amplitudes at the m nodes of the diaphragm-fluid interface. Elements of $\{\delta_0\}$ are real. The pressure in the fluid medium is then represented by

$$\{p\} = \{p_0\} e^{j\omega t} \quad (15)$$

where $\{p_0\}$ is a $k \times 1$ vector of pressure amplitudes (complex) at the k nodes of the region.

Inserting Eqs. (14) and (15) into Eq. (4) gives

$$([H] - \omega^2 [Q] + j\omega [D])\{p\} = \omega^2 \{B\} \quad (16)$$

where $\{B\} = [L]^T \{\delta_0\}$.

In the computer program, the system matrices $[H]$, $[Q]$, $[D]$, and $\{B\}$ are assembled from the contributions of each individual finite element in various subroutines. Since only a small number of nodes are located on the non-reflection boundary, the matrix $[D]$ is sparse. In order to reduce computer storage requirements, $[D]$, which is symmetric, is stored as three vectors: the principal diagonal and the two diagonals immediately above. At the same time, the approximated spherical contribution $\frac{c}{r}[D]$ at the

non-reflection boundary is computed. These quantities are real and are added directly to the matrix [H] in the appropriate locations.

The final subroutine introduces the value of omega and multiplies the matrices [Q], [D], and {B} by the appropriate power of omega before the left-hand side is summed to form one complex matrix. Thus the system of equations is reduced to

$$[S]\{p\} = \{F\} \quad (17)$$

where [S] is a $k \times k$ complex matrix and {F} is a column vector of order $k \times 1$ in which only m elements are nonzero.

The complex pressure amplitudes in Eq. (17) are found by using the Gaussian elimination and back substitution method.

The absolute value of the pressure and the phase angle are calculated in the program and printed out in array form. Additionally, a system energy balance and the diaphragm acoustic impedance are determined.

The program provides for multiple-problem solution by using incremented values of omega so that a range of frequencies can be studied.

VI. RESULTS

Problems studied were chosen to verify the accuracy of the method through comparison with available, exact (analytic) solutions. Results for each problem are discussed below.

Problem 1. Piston in a Rigid Tube

To verify the correctness of the computer program, finite element solutions were obtained for the problem of a harmonically oscillating circular piston at one end of a fluid-filled, rigid pipe of equal diameter. An infinite length was simulated by terminating the finite element region with a plane non-reflection boundary at a distance of one piston diameter. This is, of course, a one dimensional problem with uniform pressure amplitude throughout and phase angle is a linear function of distance along the pipe.

Detailed results are not presented for this essentially trivial test problem. It was found, however, that there was excellent agreement with theory for long wave-lengths. For wave-lengths less than approximately four times the element width (measured parallel to the direction of wave propagation), the accuracy deteriorated. This is understandable, since the shape functions employed represent the instantaneous pressure profile across an element by a parabolic arc. The lower limit on wave-length corresponds,

for a given element grid, to an upper limit on frequency.

Problem 2. Piston in an Infinite Baffle

The problem explored most extensively is that of a harmonically oscillating circular piston surrounded by an infinite rigid baffle and radiating into a semi-infinite fluid region. For this problem, the radiation boundary is a hemispherical surface with the center located at the piston center and the radius is four times that of the piston. The element grid.(see Figure 4, Appendix A) contains 16 elements. It is derived by mapping a 4×4 square array from the ξ, n plane into a quadrant of a circle.

Analytic results for this problem are readily available (e.g., see [1], [4]). In Table I, the pressure amplitudes and phase angles along the z axis, obtained by the finite element method (FEM), are compared with exact results. Two sets of finite element results are given. For those designated FEM1, the spherical wave correction at the radiation boundary is included. For FEM2, the correction is omitted. Details are given in Table I for two circular frequencies, $\omega = .1$ and $.6$ rad/sec. The corresponding wave-lengths are approximately 63 ft and 10 feet.

Examination of Table I shows that FEM1 results give generally good agreement with exact results. Those for FEM2 are considerably poorer, although the discrepancies are smaller for $\omega = .6$ rad/sec. This is understandable since the $1/r$ contribution to specific acoustic impedance is relatively less important as ω increases (see Eq. (12)).

It is believed that a more refined finite element mesh (more elements) should afford significant improvement. Since the computer program for this problem required 320K bytes of core storage, it was not feasible to investigate this without major program revisions.

In predicting transducer performance the resultant fluid reaction on the piston is needed. This is normally reported in the form of piston radiation impedance, which is complex and is found by dividing the piston force by the piston velocity. The real part of the radiation impedance is called the radiation resistance and the imaginary part is called the radiation reactance.

Table II provides a comparison with exact values for the radiation resistance and reactance. Results are given for FEM1 and FEM2 over a range of frequencies. Again it is observed that the spherical correction significantly improves the results. Note that the radiation resistance obtained by FEM1 continues to give good results through $\omega = .9$ rad/sec.

Computer solutions of this problem were obtained for a range of frequency from $\omega = .1$ rad/sec to $\omega = 1.2$ rad/sec by .1 rad/sec increments. Comparisons at the upper end of this range are omitted from Tables I and II because the departure from exact results does not permit useful employment of the finite element method without grid refinement. Complete computer results for pressure amplitude, phase

TABLE I
PRESSURE AMPLITUDE AND PHASE ANGLE ON AXIS

ω rad/sec	z ft	PRESSURE AMPLITUDE			PHASE ANGLE		
		EXACT lb/ft ²	FEM1 lb/ft ²	FEM2 lb/ft ²	EXACT deg	FEM1 deg	FEM2 deg
.1	0	.01997	.02061	.01794	-5.7	-5.7	-11.6
.1	2	.00828	.00889	.00676	-13.8	-13.1	-31.9
.1	4	.00472	.00469	.00376	-24.3	-24.9	-68.3
.1	6	.00325	.00329	.00337	-35.3	-35.8	-92.1
.1	8	.00246	.00247	.00334	-46.5	-47.4	-107.3
.6	0	.678	.699	.625	-34.4	-33.2	-34.7
.6	2	.295	.300	.273	-83.0	-78.7	-89.2
.6	4	.169	.172	.186	-145.6	-145.4	-150.5
.6	6	.117	.116	.106	-211.8	-211.0	-210.6
.6	8	.089	.086	.084	-279.3	-279.2	-289.3

TABLE II
PISTON RADIATION RESISTANCE AND REACTANCE

ω rad/sec	RESISTANCE			REACTANCE		
	EXACT lb.sec ft	FEM1 lb.sec ft	FEM2 lb.sec ft	EXACT lb.sec ft	FEM1 lb.sec ft	FEM2 lb.sec ft
.1	.249	.254	.451	2.11	2.06	1.68
.2	.979	.978	.687	4.09	3.97	3.56
.3	2.13	2.12	1.43	5.81	5.65	5.83
.4	3.61	3.62	3.75	7.18	6.99	8.11
.5	5.32	5.34	6.75	8.13	7.87	7.43
.6	7.12	7.12	6.61	8.62	8.31	7.00
.7	8.89	8.87	7.50	8.67	8.35	8.72
.8	10.51	10.53	10.89	8.32	7.99	9.59
.9	11.90	11.97	13.60	7.64	7.24	6.69

FEM1 - Finite element results with spherical correction.
FEM2 - Finite element results without spherical correction.

Phase angle given is for pressure relative to piston displacement.

Fluid density = 1 lb.sec/ft⁴ Piston Radius = 2 ft.

Acoustic Velocity = 1 ft/sec. Piston Amplitude = 1 ft.

angle, and impedance components at several frequencies are given in Appendix A.

Problem 3. Parabolic Diaphragm in an Infinite Baffle

This problem, a modification of the previous problem, replaces the piston by a circular diaphragm having a fixed edge and having a deflection surface in the form of a paraboloid of revolution. Study of this problem was undertaken in an effort to improve agreement in the energy balance check (discussed below) incorporated into the program. It was believed that elimination of fluid velocity discontinuity at the edge of the piston in problem 1 might result in a significant improvement.

Analytic results for this problem are not available in standard acoustic texts, but conventional techniques can be utilized to obtain the pressure p along the z axis in complex form as

$$p = \frac{2j\rho c^3 \delta_0}{\omega a^2} \left[\left(1 + j \frac{\omega s}{c} \right) e^{-j \frac{\omega s}{c}} - \left(1 + \frac{\omega^2 a^2}{2c^2} + j \frac{\omega z}{c} \right) e^{-j \frac{\omega z}{c}} \right] e^{j\omega t} \quad (18)$$

where

δ_0 = displacement amplitude at diaphragm center

a = diaphragm diameter

s = "slant" distance = $(z^2 + a^2)^{\frac{1}{2}}$

For this problem only a single finite element solution (FEM3) was obtained. The spherical correction is included. Table III gives a comparison with exact results (Eq. (18))

TABLE III
PRESSURE AMPLITUDE AND PHASE ANGLE ON AXIS

ω rad/sec	z ft	PRESSURE AMPLITUDE		PHASE ANGLE	
		EXACT lb/ft ²	FEM3 lb/ft ²	EXACT deg	FEM3 deg
.1	0	.01322	.01427	-4.3	-4.1
.1	2	.00438	.00461	-13.1	-12.6
.1	4	.00240	.00242	-23.7	-24.2
.1	6	.00164	.00166	-34.8	-35.5
.1	8	.00124	.00125	-46.2	-47.1
.6	0	.4598	.4934	-25.7	-23.8
.6	2	.1565	.1590	-78.5	-75.5
.6	4	.0864	.0867	-142.97	-142.3
.6	6	.0589	.0584	-209.4	-209.4
.6	8	.0445	.0436	-277.8	-278.1

FEM3 - Finite element results with spherical correction.

Phase angle is for pressure relative to diaphragm displacement.

Fluid density = 1 lb.sec/ft⁴.

Acoustic velocity = 1 ft/sec.

Diaphragm radius = 2 ft.

Diaphragm amplitude (center) = 1 ft.

for pressure amplitudes and phase angles for values of

ω = .1 and .6 rad/sec.

Examination of Table III shows that agreement near the diaphragm (small values of z) is not as good as FEM1 in Table I. At the radiation boundary however, the FEM3 errors are comparable to those for FEM1.

Energy Balance Check

Prior experience, by others, suggested that an energy balance check would be a useful feature of a finite element program. Specifically, since solutions represent steady-state behavior, the input power, averaged over a cycle, should equal the corresponding average value of the output power. Input occurs at the piston, or diaphragm, and output at the radiation boundary. Expressions for these quantities are derived and incorporated in the computer program.

A number of program errors in the energy balance calculations (Appendix B) prevented valid results until the final stage of the investigation. Thus, the values of average power in and average power out are not included in the computer output (Appendix A). Recent computations, with program errors corrected, have shown excellent agreement of these quantities to at least six significant digits in the lower range of the circular frequency. Even at higher frequencies, where solution accuracy (pressure amplitudes and phase angles) deteriorates markedly, five significant digit agreement is maintained.

VII. CONCLUSIONS

It has been shown that the finite element method can provide acceptable results concerning generation and propagation of acoustic waves. The parabolic iso-parametric element provides an economical, accurate means of representing regions having curved boundaries.

The principal limitation of the method is evident from the empirically deduced results that, for acceptable accuracy, a single element must not span more than one-quarter wave-length. For wave-lengths of the order of magnitude of the piston radius, the number of nodes required would be around 900. For the present program, which already utilizes 320K bytes of core storage for 65 nodes, this is far beyond capability.

APPENDIX A
COMPUTER OUTPUT

The rows of pressures and phase angles shown in the computer output correspond to the numbering system shown on the finite element region, Figure 4.

The zeros printed in the array of pressures and phase angles do not indicate computed values, but facilitate printing the output in array form.

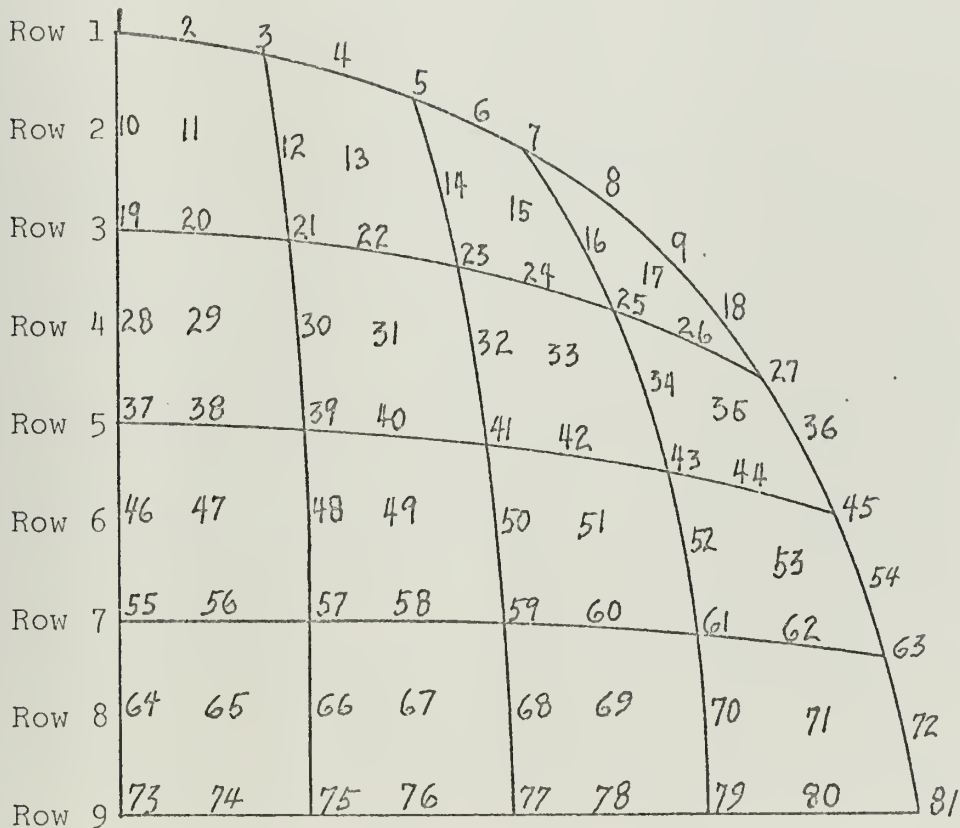


Figure 4. Format for Pressure and Phase Angle Array.

The output data are arranged according to the following sequence.

- FEM1. Piston in infinite baffle with spherical correction added at the non-reflection boundary.
- FEM2. Piston in infinite baffle without spherical correction added at the non-reflection boundary.
- FEM3. Diaphragm in infinite baffle with spherical correction added at the non-reflection boundary.

COMPUTER OUTPUT-GENERAL

TITLE OF GRAPH OF CORNER NODE POINTS TO BE PLOTTED
 GRAPH ILLUSTRATING SYSTEM CORNER NODE LOCATIONS
 FINITE ELEMENT STUDY OF ACOUSTIC WAVES...D.DEAN

NUMBER OF ELEMENTS=16

NUMBER OF NODES PER ELEMENT INCLUDING CENTER NODES= 9

NUMBER OF TOTAL SYSTEM NODES INCLUDING CENTER NODES=81

NUMBER OF NODES PER ELEMENT EXCLUDING CENTER NODES= 8

NUMBER OF SYSTEM NODES EXCLUDING CENTER NODES=65

MAIN NODE NO	X COORD	Y COORD
1	0.0	0.0
2	4.000000	0.0
3	8.000000	0.0
4	7.39103	3.06146
5	5.65585	5.65685
6	3.06146	7.39103
7	0.0	8.00000
8	0.0	4.00000

NUMBER OF ELEMENT DIVISIONS IN X DIRECTION= 4

NUMBER OF ELEMENT DIVISIONS IN THE Y DIRECTION= 4

ASSIGNMENT OF NODE NUMBERS TO ELEMENTS

ELEMENT NO	NODE NUMBERS (8 NODDED ELEMENTS)
1	15 16 17 14 3 2
2	17 18 19 12 5 4
3	21 20 21 13 7 6
4	29 30 31 23 14 9
5	31 32 33 25 12 17
6	33 34 35 26 19 18
7	35 36 37 27 21 20
8	43 44 45 28 23 22
9	45 46 47 39 31 30
10	47 48 49 40 33 32
11	49 50 51 41 35 34
12	50 51 52 42 37 36
13	57 58 59 45 46 47
14	59 60 61 54 47 48
15	61 62 63 55 49 50
16	63 64 65 56 51 50

COMPUTER OUTPUT-GENERAL

VALUES OF XI AND ETA FOR WHICH X AND Y COORDINATES WILL BE CALCULATED

VALUES OF X AND Y		(X COORDINATES ON TOP-Y COORDINATES ON BOTTOM)								
		1	2	3	4	5	6	7	8	9
VALUES OF XI	VALUES OF ETA									
1	-1.00000	0.00000	1.00000	1.00000	3.06146	3.75400	4.41741	5.05170	5.65685	5.65685
2	-0.75000	0.75000	0.00000	1.58899	2.33979	7.06297	6.66459	6.19588	5.65685	5.65685
3	-0.50000	0.50000	0.25000	7.83617	7.64876	7.39103	7.06297	6.66459	6.19588	5.65685
4	-0.25000	0.25000	0.00000	1.70190	2.51462	3.30185	4.06359	4.79984	5.51061	6.19588
5	0.00000	0.25000	0.50000	6.88213	6.73090	6.51813	6.24382	5.90798	5.51061	5.05170
6	0.25000	0.50000	0.75000	5.92082	5.80211	5.63066	5.40647	5.12953	5.90798	5.66459
7	0.50000	0.75000	0.994659	4.95224	4.86240	4.72863	4.55090	4.32922	4.06359	4.41741
8	0.75000	0.994809	0.99486	3.93515	2.88087	3.81203	4.72863	5.63066	6.24382	7.06297
9	1.00000	0.994978	0.99498	3.97634	3.91177	3.81203	3.67713	3.50707	3.06297	3.75400

COMPUTER OUTPUT-GENERAL

NUMBER OF NODES ON NONREFLECTION BOUNDARY=17
NONREFLECTION BOUNDARY ALONG TOP OF ELEMENT IS FROM $XI=-1.00$ TO $XI=1.00$
NONREFLECTION BOUNDARY ALONG RIGHT SIDE OF ELEMENT IS FROM $ETA=1.00$ TO $ETA=-1.00$
NODE NUMBERS LOCATED ON THE NONREFLECTION BOUNDARY

37

1	7
2	8
3	9
4	14
5	23
6	28
	42
	51
	56
	65

SPEED OF SOUND = 1.00000

DENSITY OF FLUID= 1.00000

NUMBER OF NODES IN CONTACT WITH PISTON= 3

RANGE ON LEFT BOUNDARY WHICH PISTON IS IN CONTACT IS FROM $ETA=-0.50$ TO $ETA=-1.00$

NODE NUMBERS IN CONTACT WITH FORCING FUNCTION

43
52
57

AMPLITUDE OF PISTON AT THE INTERFACE NODES

NODE	AMPLITUDE
43	1.0000000
52	1.0000000
57	1.0000000

INITIAL VALUE OF OMEGA= 0.10000

INCREMENT VALUE OF OMEGA= 0.10000

NUMBER OF INCREMENTS OF OMEGA=12

FEM1. Piston in Infinite Baffle with Spherical Connection
 VALUE OF OMEGA FOR THIS RUN= 0.10000
 ABSOLUTE VALUE AND PHASE ANGLE OF PRESSURE
 (PRESSURE ON TOP-PHASE ANGLE ON BOTTOM)

0.00253 -45.990	0.00254 -45.842	0.00253 -46.006	0.00253 -46.017	0.00252 -46.136	0.00252 -46.214	0.00251 -46.317	0.00251 -46.436	0.00250 -46.628
0.00290 -40.088	0.0 0.0	0.00286 -40.722	0.0 0.0	0.00276 -42.216	0.0 0.0	0.00263 -44.241	0.0 0.0	0.00250 -46.718
0.00341 -34.109	0.00334 -34.805	0.00328 -35.467	0.00316 -36.865	0.00302 -38.494	0.00289 -40.294	0.00275 -42.368	0.00262 -44.529	0.00249 -46.870
0.00405 -28.729	0.0 0.0	0.00380 -30.605	0.0 0.0	0.00334 -34.891	0.0 0.0	0.00287 -40.608	0.0 0.0	0.00249 -47.016
0.00509 -22.841	0.00501 -23.195	0.00451 -25.837	0.00411 -28.369	0.00369 -31.626	0.00331 -35.257	0.00299 -39.147	0.00272 -43.076	0.00249 -47.123
0.00733 -15.824	0.0 0.0	0.00565 -20.573	0.0 0.0	0.00403 -28.939	0.0 0.0	0.00309 -37.837	0.0 0.0	0.00249 -47.234
0.01232 -9.420	0.00907 -12.820	0.00669 -17.413	0.00532 -21.916	0.00437 -26.705	0.00369 -31.724	0.00318 -36.860	0.00280 -42.074	0.00250 -47.289
0.01858 -6.260	0.0 0.0	0.00777 -15.019	0.0 0.0	0.00463 -25.239	0.0 0.0	0.00324 -36.232	0.0 0.0	0.00251 -47.320
0.02061 -5.651	0.01175 -9.930	0.00889 -13.111	0.00621 -18.791	0.00469 -24.919	0.00385 -30.488	0.00329 -35.746	0.00282 -41.573	0.00247 -47.442
ACOUSTIC IMPEDANCE								
REAL=	0.25423472							
IMAG=	2.05667215							

FEM1. Piston in Infinite Baffle with Spherical Correction
Added at the Non-Reflection Boundary

VALUE OF OMEGA FOR THIS RUN= 0.30000

ABSOLUTE VALUE AND PHASE ANGLE OF PRESSURE
(PRESSURE ON TOP-PHASE ANGLE ON BOTTOM)

0.02178	0.02174	-136.276	-136.498	0.02177	-136.673	0.02174	-136.943	0.02174	-137.175	0.02175	-137.462	0.02176	-137.781	0.02177	-138.320
0.02481	0.0	0.0	-120.845	0.02450	0.0	0.0	-125.201	0.02378	0.0	0.0	-131.196	0.02284	0.0	0.0	-138.559
0.02897	0.02876	-102.948	-105.131	0.02808	-109.152	0.02722	-113.958	0.02620	-119.366	0.02508	-125.519	0.02398	-131.990	0.02287	-138.987
0.03496	0.0	0.0	-90.291	0.03290	0.0	0.0	-103.182	0.02897	0.0	0.0	-120.241	0.02509	0.0	0.0	-139.374
0.04404	0.04289	-68.438	-75.919	0.03933	-83.632	0.03572	-93.411	0.03213	-104.217	0.02893	-115.755	0.02620	-127.552	0.02384	-139.704
0.06255	0.0	0.0	-60.614	0.04889	0.0	0.0	-85.250	0.03547	0.0	0.0	-111.874	0.02719	0.0	0.0	-139.998
0.10619	0.07915	-37.559	-51.048	0.05916	-64.366	0.04714	-78.518	0.03866	-93.566	0.03255	-108.899	0.02803	-124.498	0.02462	-140.164
0.16362	0.0	0.0	-44.035	0.06930	0.0	0.0	-74.283	0.04110	0.0	0.0	-106.979	0.02862	0.0	0.0	-140.299
0.18304	0.10585	-28.998	-38.569	0.07853	-55.329	0.05498	-73.054	0.04205	-89.622	0.03434	-105.764	0.02888	-123.098	0.02486	-140.440

ACOUSTIC IMPEDANCE

REAL= 2.11780205

IMAG= 5.65370620

FEM1. Piston in Infinite Raffle with spherical Correction
 VALUE OF OMEGA FOR THIS RUN= 0.60000
 ABSOLUTE VALUE AND PHASE ANGLE OF PRESSURE
 (PRESSURE ON TOP-PHASE ANGLE ON BOTTOM)

0.07559	0.07613 86.954	0.07617 86.955	0.07693 86.417	0.07759 86.167	0.07835 85.708	0.07948 85.323	0.08040 84.812	0.08172 83.943
0.08637	0.0 0.0	0.08608 117.825	0.0 0.0	0.08540 109.550	0.0 0.0	0.08432 97.978	0.0 0.0	0.08282 83.676
0.09955	0.10061 156.262	0.09853 149.116	0.09735 141.666	0.09547 132.479	0.09262 121.592	0.09021 109.661	0.08687 96.811	0.08416 83.067
0.12293	0.0 -168.583	0.11745 179.914	0.0 0.0	0.10695 153.794	0.0 0.0	0.09566 120.244	0.0 0.0	0.08505 82.491
0.15587	0.14923 -133.372	0.14403 -150.744	0.13192 -167.172	0.12155 173.329	0.11097 152.061	0.10184 129.651	0.09312 106.141	0.08592 81.974
0.21095	0.0 -93.934	0.17615 -122.376	0.0 0.0	0.13770 -170.201	0.0 0.0	0.10732 137.294	0.0 0.0	0.08690 81.489
0.36675	0.28723 -75.328	0.22673 -102.174	0.18449 -128.915	0.15359 -157.248	0.13028 173.449	0.11200 143.391	0.09811 112.580	0.08750 81.173
0.60717	0.0 -36.413	0.27351 -88.602	0.0 0.0	0.16594 -148.976	0.0 0.0	0.11558 147.324	0.0 0.0	0.08829 80.855
0.69899	0.42606 -33.217	0.30000 -78.874	0.21718 -112.362	0.17233 -145.348	0.14117 -177.879	0.11589 148.974	0.09995 115.227	0.08645 80.824

ACOUSTIC IMPEDANCE
 REAL= 7.11911492
 IMAG= 8.30592614

FEM1. Piston in Infinite Baffle with Spherical Correction
Added at the Non-Reflection Boundary

VALUE OF OMEGA FOR THIS RUN= 0.90000

ABSOLUTE VALUE AND PHASE ANGLE OF PRESSURE
(PRESSURE ON TOP-PHASE ANGLE ON BOTTOM)

0.13355 -48.071	0.13613 -47.932	0.13579 -48.529	0.13968 -48.529	0.14245 -49.115	0.14650 -50.453	0.15661 -51.005	0.16354 -53.654
0.15353 -4.213	0.0.0 -1.440	0.15462 -1.440	0.0.0 -0.0	0.15841 -14.777	0.0.0 -0.0	0.16390 -32.507	0.0.0 -54.061
0.17814 56.454	0.17905 54.050	0.17866 45.619	0.17980 33.786	0.18045 20.005	0.18019 2.857	0.18079 -14.822	0.17760 -34.395
0.22101 109.867	0.0.0 0.0	0.21494 91.552	0.0.0 0.0	0.20761 50.888	0.0.0 0.0	0.19663 0.578	0.0.0 -55.698
0.28014 162.646	0.27153 153.347	0.26876 136.330	0.25401 109.466	0.24446 80.474	0.22875 47.889	0.21540 14.864	0.18977 -20.367
0.35583 -142.184	0.0.0 0.0	0.32268 175.666	0.0.0 0.0	0.28309 104.587	0.0.0 0.0	0.23312 0.25.969	0.0.0 -56.922
0.63930 -79.378	0.54709 -111.828	0.46567 -151.062	0.38422 167.994	0.32637 124.652	0.28326 79.864	0.24769 35.119	0.21827 -10.397
1.20887 -53.483	0.0.0 0.0	0.59822 -131.342	0.0.0 0.0	0.36241 136.976	0.0.0 0.0	0.25955 40.911	0.0.0 -57.750
1.46254 -49.631	0.97506 -85.219	0.63836 -118.876	0.48057 -168.541	0.37286 143.663	0.31430 93.398	0.26065 0.43.164	0.22686 -6.174

ACOUSTIC IMPEDANCE

REAL= 11.96803122
IMAG= 7.24443414

0.19239
-58.558

FEM2. Piston in Infinite Baffle Without Spherical Correction
 VALUE OF OMEGA FOR THIS RUN= 0.10000
 ABSOLUTE VALUE AND PHASE ANGLE OF PRESSURE
 (PRESSURE ON TOP-PHASE ANGLE ON BOTTOM)

0.00336 -104.805	0.00335 -104.666	0.00335 -104.877	0.00335 -104.952	0.00335 -105.151	0.00335 -105.318	0.00335 -105.517	0.00335 -105.741	0.00335 -106.040
0.00336 -98.047	0.0 0.0	0.00336 -98.930	0.0 0.0	0.00335 -100.924	0.0 0.0	0.00335 -103.435	0.0 0.0	0.00334 -106.234
0.00340 -88.884	0.00339 -90.120	0.00338 -91.277	0.00337 -93.588	0.00336 -96.099	0.00335 -98.663	0.00335 -101.366	0.00334 -103.939	0.00334 -106.480
0.00353 -77.901	0. 0.0	0.00347 -82.123	0. 0.0	0.00338 -90.469	0. 0.0	0.00335 -99.231	0. 0.0	0.00334 -106.708
0.00396 -62.364	0.00391 -63.401	0.00369 -70.759	0.00355 -77.149	0.00344 -84.376	0.00338 -91.204	0.00335 -97.300	0.00334 -102.433	0.00334 -106.878
0.00547 -40.418	0. 0.0	0.00427 -55.516	0. 0.0	0.00352 -78.541	0. 0.0	0.00335 -95.428	0. 0.0	0.00334 -107.024
0.00990 -21.154	0.00692 -31.017	0.00497 -45.494	0.00407 -59.634	0.00363 -73.085	0.00343 -84.648	0.00336 -93.930	0.00334 -101.277	0.00334 -107.089
0.01595 -13.011	0. 0.0	0.00581 -37.842	0. 0.0	0.00373 -69.199	0. 0.0	0.00336 -92.929	0. 0.0	0.00334 -107.128
0.01794 -11.564	0.00936 -22.554	0.00676 -31.885	0.00462 -49.896	0.00376 -68.341	0.00347 -82.022	0.00337 -92.074	0.00334 -100.682	0.00334 -107.263
ACOUSTIC IMPEDANCE								
REAL= 0.45053255								
IMAG= 1.68881084								

FEM2 . Piston in Infinite Baffle Without Spherical Correction
 VALUE OF OMEGA FOR THIS RUN= 0.30000
 ABSOLUTE VALUE AND PHASE ANGLE OF PRESSURE
 (PRESSURE ON TOP-PHASE ANGLE ON BOTTOM)

-0.01798	0.01793	0.01796	0.01793	0.01792	0.01790	0.01788	0.01785	0.01784
-144.904	-144.753	-145.027	-145.273	-145.624	-145.937	-146.307	-146.713	-147.337
0.01810	0.0	0.01805	0.0	0.01795	0.0	0.01786	0.0	0.01789
-125.114	0.0	-127.452	0.0	-132.844	0.0	-139.799	0.0	-147.655
0.01959	0.01949	0.01909	0.01871	0.01835	0.01806	0.01791	0.01781	0.01779
-100.100	-102.660	-105.856	-111.655	-118.391	-125.608	-133.295	-140.764	-148.153
0.02430	0.0	0.02236	0.0	0.01945	0.0	0.01800	0.0	0.01777
-75.714	0.0	-83.713	0.0	-102.782	0.0	-126.700	0.0	-148.599
0.03414	0.03293	0.02866	0.02485	0.02153	0.01932	0.01821	0.01781	0.01775
-53.351	-54.844	-63.818	-73.985	-88.003	-104.117	-120.662	-135.724	-148.960
0.05583	0.0	0.03971	0.0	0.02441	0.0	0.01847	0.0	0.01774
-33.246	0.0	-46.246	0.0	-75.995	0.0	-115.134	0.0	-149.232
0.10358	0.07417	0.05134	0.03723	0.02759	0.02167	0.01876	0.01784	0.01772
-18.598	-25.978	-37.069	-50.025	-66.867	-87.835	-110.709	-131.895	-149.440
0.16325	0.0	0.06278	0.0	0.03018	0.0	0.01902	0.0	0.01771
-12.217	0.0	-31.053	0.0	-61.282	0.0	-107.811	0.0	-149.440
0.18311	0.10276	0.07324	0.04636	0.03115	0.02309	0.01908	0.01784	0.01773
-11.038	-19.634	-26.699	-40.885	-59.783	-81.850	-105.829	-130.124	-149.601

ACOUSTIC IMPEDANCE
 REAL= 1.42595320
 IMAG= 5.822615666

FEM2 . Piston in Infinite Baffle Without Spherical Correction
 Added at the Non-Reflection Boundary

VALUE OF OMEGA FOR THIS RUN=	0.60000
ABSOLUTE VALUE AND PHASE ANGLE OF PRESSURE (PRESSURE ON TOP-PHASE ANGLE ON BOTTOM)	
0.07266	0.07322 75.183
0.07526	0.0 113.624
0.09072	0.09118 153.276
-0.12570	0.0 -169.876
-0.16452	-0.15811 -144.033
-0.20198	0.0 -105.068
0.311905	0.25874 -85.177
0.53874	0.0 -38.377
0.62510	0.37118 -34.649
ACOUSTIC IMPEDANCE	
REAL =	6.60598018
IMAG =	6.99861861

FEM2. Piston in Infinite Baffle Without Spherical Correction
Added at the Non-Reflection Boundary

VALUE OF OMEGA FOR THIS RUN= 0.90000

A3SOLUTE VALUE AND PHASE ANGLE OF PRESSURE
(PRESSURE ON TOP-PHASE ANGLE ON BOTTOM)

0.14431	0.14672	0.14637	0.15017	0.15273	0.15675	0.16209	0.16658	0.17368
-53.197	-52.175	-53.027	-53.632	-54.224	-55.581	-56.141	-57.417	-58.849
0.15527	0.0	0.15551	0.0	0.15868	0.0	0.16676	0.0	0.17922
4.211	-2.094	-2.094	0.0	-17.075	0.0	-36.728	0.0	-59.282
0.19974	0.19974	0.19571	0.19144	0.18594	0.18015	0.17929	0.17998	0.18731
58.374	56.119	48.170	36.540	22.225	3.375	-16.747	-38.681	-59.978
0.24969	0.0	0.24654	0.0	0.22950	0.0	0.19575	0.0	0.19235
105.800	0.0	89.399	0.0	53.048	0.0	0.0.933	0.0	-60.975
0.28526	0.27934	0.28405	0.28240	0.27807	0.25105	0.21948	0.19803	0.19796
159.428	149.237	131.313	105.178	79.220	49.966	16.786	-22.890	-61.400
0.38208	0.0	0.33235	0.0	0.31326	0.0	0.24385	0.0	0.20267
-140.381	0.0	174.968	0.0	100.366	0.0	28.377	0.0	-62.090
0.71787	0.62007	0.49012	0.37796	0.34305	0.31944	0.26506	0.21600	0.20493
-83.015	-111.521	-148.131	166.954	119.408	78.005	37.436	-11.265	-62.402
1.29487	0.0	0.66050	0.0	0.36737	0.0	0.28154	0.0	0.20818
-58.602	0.0	-128.609	0.0	132.192	0.0	42.900	0.0	-62.657
1.55387	1.10882	0.72188	0.48296	0.37122	0.34985	0.28443	0.22566	0.20580
-54.747	-88.011	-117.150	-165.799	139.523	89.706	45.091	-6.520	-63.550

ACOUSTIC IMPEDANCE

REAL= 13.60456934
IMAG= 6.68581093

NUMBER OF INCREMENTS OF OMEGA=12

FEM3. Diaphragm in Infinite Baffle with
Spherical Contribution Added at
the Non-Reflection Boundary

VALUE OF OMEGA FOR THIS RUN= 0.10000

ABSOLUTE VALUE AND PHASE ANGLE OF PRESSURE
(PRESSURE ON TOP-PHASE ANGLE ON BOTTOM)

0.000126 -46.066	0.00127 -46.009	0.00126 -46.082	0.000126 -46.125	0.000126 -46.201	0.000126 -46.253	0.000126 -46.325	0.000126 -46.401	0.000126 -46.553
0.000145 -40.277	0.0 0 0.0	0.00142 -40.861	0.0 0 0.0	0.000138 -42.263	0.0 0 0.0	0.000132 -44.206	0 0 0.0	0.000125 -46.607
0.000169 -34.393	0.000167 -34.906	0.000163 -35.646	0.000158 -36.926	0.000151 -38.500	0.000145 -40.263	0.000138 -42.288	0.000132 -44.416	0.000125 -46.729
0.000202 -28.783	0.0 0 0.0	0.000190 -30.623	0.0 0 0.0	0.000167 -34.859	0.0 0 0.0	0.000144 -40.492	0 0 0.0	0.000125 -46.834
0.000255 -22.849	0.000247 -23.542	0.000227 -25.719	0.000206 -28.296	0.000185 -31.592	0.000166 -35.131	0.000150 -38.961	0.000137 -42.883	0.000125 -46.928
0.000351 -16.563	0.0 0 0.0	0.000281 -20.740	0.0 0 0.0	0.000204 -28.695	0.0 0 0.0	0.000156 -37.633	0 0 0.0	0.000126 -47.002
0.000563 -10.325	0.000454 -12.815	0.000340 -17.136	0.000271 -21.541	0.000221 -26.423	0.000186 -31.460	0.000161 -36.599	0.000141 -41.822	0.000126 -47.042
0.01060 -5.490	0.0 0 0.0	0.000407 -14.325	0.0 0 0.0	0.000235 -24.849	0.0 0 0.0	0.000164 -35.925	0 0 0.0	0.000127 -47.070
0.01427 -4.084	0.000689 -8.472	0.000461 -12.642	0.000317 -18.450	0.000242 -24.176	0.000196 -29.994	0.000166 -35.525	0.000142 -41.336	0.000125 -47.116

ACOUSTIC IMPEDANCE

REAL= 0.06370248
IMAG= 0.63658158

FEM3. Diaphragm in Infinite Baffle with Spherical Contribution
Added at the Non-Reflection Boundary

VALUE OF OMEGA FOR THIS RUN= 0.30000

ABSOLUTE VALUE AND PHASE ANGLE OF PRESSURE
(PRESSURE ON TOP-PHASE ANGLE ON BOTTOM)

-0.01098	0.01099	0.01098	0.01098	0.01098	0.01098
-136.759	-136.686	-136.789	-136.962	-137.141	-137.291
-0.01254	0.0	0.01238	0.0	0.0	0.0
-119.497	0.0	-121.205	0.0	-125.339	-131.107
-0.01463	-0.01451	-0.01418	-0.01374	-0.01323	-0.01277
-101.915	-103.289	-105.574	-109.335	-113.990	-119.283
-0.01762	0.0	0.01660	0.0	0.0	0.0
-84.934	0.0	-90.420	0.0	-103.097	-119.916
-0.02220	0.02150	0.01987	0.01805	0.01624	0.01462
-67.248	-69.403	-75.697	-83.460	-93.262	-103.847
0.03950	0.0	0.02459	0.0	0.0	0.0
-48.708	0.0	-61.047	0.0	-84.587	-111.289
0.04919	0.03997	0.03023	0.02404	0.01961	0.01648
-30.231	-37.565	-50.239	-63.295	-77.811	-92.797
0.09381	0.0	0.03635	0.0	0.0	0.0
-16.037	0.0	-42.030	0.0	-73.145	-106.142
0.12726	0.06189	0.04096	0.02817	0.02092	0.01447
-11.928	-24.759	-37.151	-54.245	-71.068	-88.328

ACOUSTIC IMPEDANCE
REAL= 0.54011493
IMAG= 1.80323806

0.01100
-138.120

0.01100
-138.254

0.01100
-138.590

0.01100
-138.656

0.01100
-139.656

FEM3. Diaphragm in Infinite Baffle with Spherical Contribution
Added at the Non-Reflection Boundary

VALUE OF OMEGA FOR THIS RUN=	0.60000
ABSOLUTE VALUE AND PHASE ANGLE OF PRESSURE (PRESSURE ON TOP-PHASE ANGLE ON BOTTOM)	
0.04011 86.160	0.04037. 86.264.
0.04589 120.534	0.04555 117.261
0.05313 155.411	0.05217 148.517
0.06475 -169.810	0.06160 179.198
0.08137 -134.539	0.07902 -139.386
0.11005 -98.250	0.09217 -122.886
0.17825 -60.629	0.11776 -100.607
0.35379 -32.026	0.14360 -84.780
0.49338 -23.844	0.24710 -49.582
ACOUSTIC IMPEDANCE	
REAL=	1.92789152
IMAG=	2.94996724

FEM3. Diaphragm in Infinite Baffle with Spherical Contribution
Added at the Non-Reflection Boundary

VALUE OF OMEGA FOR THIS RUN=	0.90000
ABSOLUTE VALUE AND PHASE ANGLE OF PRESSURE (PRESSURE ON TOP-PHASE ANGLE ON BOTTOM)	
0.07730	0.07845 -49.379
0.08865	0.0 0.0
0.10270	0.10326 54.794
0.12664	0.0 106.954
0.15738	0.15560 159.354
0.20929	0.0 -147.999
0.33963	0.29929 -89.983
0.72350	0.0 -47.294
1.05780	0.55984 -35.353
ACOUSTIC IMPEDANCE	
REAL=	3.57037792
IMAG=	3.14224531

APPENDIX B - COMPUTER PROGRAM
THE FINITE ELEMENT STUDY OF ACOUSTIC WAVES CREATED BY
A MECHANISM ACTING ON A FLUID SUBSTANCE AT THE CENTER
OF AN INFINITE WALL. THE MECHANISM MAY BE A PISTON,
DIAPHRAGM, OR SOME OTHER MECHANICAL MEANS OF APPLYING
A FORCE TO THE FLUID. THE FLUID REGION AWAY FROM THE
WALL IS CONSIDERED TO BE INFINITE.

THIS PROGRAM IS DESIGNED TO TAKE ONE 8-NODED ELEMENT
AND SUBDIVIDE IT INTO ANY NUMBER OF SMALLER ELEMENTS
BY SPECIFYING THE NUMBER OF DIVISIONS DESIRED IN BOTH
THE X AND Y DIRECTIONS. EACH SUBDIVIDED ELEMENT WILL
AUTOMATICALLY BE ASSIGNED 9 GLOBAL NODE NUMBERS, 8 OF
WHICH ARE ON THE BOUNDARY AND THE 9TH IS LOCATED AT
THE CENTER. THE 9TH (CENTER) NODE IS USED TO PROVIDE
A MEANS FOR FORMULATING LEGIBLE OUTPUT. COORDINATES
OF ALL GLOBAL NODES ARE THEN CALCULATED AND PLOTTED
TO FORM THE FINITE ELEMENT MESH FOR THE PROBLEM TO BE
SOLVED. NON-REFLECTING BOUNDARY NODE NUMBERS AND THEIR
NODE NUMBERS IN CONTACT WITH THE FORCING MECHANISM ARE
AUTOMATICALLY ASSIGNED IN THE PROGRAM.

-----DATA CARDS FOR SUBROUTINE INPUT

- (1) TITLE OF GRAPH OF THE FINITE ELEMENT MESH WHICH
WILL BE GENERATED AND PLOTTED IN THE PROGRAM.
(TWO CARDS) FORMAT(6A8) TITLE OF GRAPH
- (2) NUMBER OF FLUID ELEMENTS, NUMBER OF NODES PER
ELEMENT AND TOTAL NUMBER OF SYSTEM NODES. EACH
ELEMENT HAS 8 NODES ON THE BOUNDARY AND
ONE MIDDLE NODE. THE MIDDLE NODE IS USED ONLY
TO ASSIST IN PRINTING OUT THE RESULTS IN ARRAY FORM.
(ONE CARD) FORMAT(3I10)NE,NT,NNOD
- (3) X AND Y COORDINATES OF THE EIGHT MAIN NODES
ASSIGNED TO THE BOUNDARY OF THE REGION TO BE
STUDIED. (ONE CARD PER NODE)
FORMAT(12.2F10.5) K, XM(K), YM(K)
- (4) NUMBER OF SUBDIVISIONS REQUIRED OF THE TOTAL
REGION IN BOTH THE X AND Y DIRECTION. (ONE CARD)
FORMAT(2I5) NXDIV,NYDIV
- (5) TOTAL NUMBER OF NODES LOCATED ON THE NON-REFLECTION
BOUNDARY INCLUDING TWO VALUES OF XI DEFINING THE

RANGE OF THE NON-REFLECTION BOUNDARY ALONG THE
FACE ETA=1 AND THE TWO VALUES OF ETA WHICH DEFINE
THE RANGE OF THE NON-REFLECTION BOUNDARY ALONG
THE FACE XI=1 (ONE CARD)
FORMAT(12,8X,4F10.5)NRBN,XI1,XI2,ETA1,ETA2

(6) SPEED OF SOUND AND THE FLUID DENSITY
(ONE CARD) FORMAT(2F10.5)SOUND,FLDEN

(7) NUMBER OF NODES IN WHICH THE FORCING MECHANISM
IS IN CONTACT AND TWO VALUES OF ETA DEFINING THE
RANGE OF THE FORCING MECHANISM ACTING ON THE
FACE XI=-1 (ONE CARD)
FORMAT(12,8X,2F10.5)NP,ETA1,ETA2

(8) AMPLITUDE OF THE FORCING FUNCTION AT THE NODES
WITH WHICH THE FORCING MECHANISM IS IN CONTACT.
AMPLITUDES READ FROM THE TOP DOWNWARD.
(ONE CARD) FORMAT(9F8.4)(AMP(I),I=1,NP)

(9) INITIAL VALUE OF OMEGA FOR WHICH PROBLEM IS TO
BE SOLVED, INCREMENT OF OMEGA FOR SUCCESSIVE
SOLUTIONS; AND TOTAL NUMBER OF SOLUTIONS REQUIRED.
(ONE CARD) FORMAT(2F10.5,I12)OMEGA,OINCR,NO

```
CALL INPUT
CALL HQFORM
CALL FDAMP
CALL FORCE
CALL PROB
STOP
END
```

SUBROUTINE INPUT

```
IMPLICIT COMPLEX*16 (D),REAL*8 (A-C,E-H,O-Z)
REAL*8 ITITLE
COMMON DSUM(81,81),DB(81),H(81,81),Q(81,81),B(81,81),X(81),Y(81),HE(8,8),QE(8,8)
COMMON RD(50),RDS(50),RDSS(50),XM(8),YM(8),AMP(25)
COMMON GA(4),GH(4),SF(8),XD(8),YD(8),XXD(8),YYD(8),AJ(2,2),BL(3,3)
COMMON SOUND,FLDEN,OMEGA,OINCR
COMMON NN(100,8),NDAMP(50),NPN(50),NN9(50,9),NOW(100)
COMMON NM,NNOD,NNODT,NC
COMMON /TITLE/TITLE(12),NRBN,NO,NNODT,NC
```



```

C C TITLE OF GRAPH ON WHICH CORNER NODE POINTS WILL BE PLOTTED
C C READ(5,142){TITLE(I),I=1,6}
C C READ(5,142){TITLE(I),I=7,12}
142 FORMAT(6A8)
WRITE(6,143)TITLE
143 FORMAT(14A)TITLE
144 WRITE(6,144)TITLE
FORMAT(4X,6A8/)

C C NUMBER OF FLUID ELEMENTS, NODES PER ELEMENT, TOTAL
C C NODES, AND NUMBER OF WORKING NODES.
C C READ(5,100)NE,MT,NNODT
100 FORMAT(3I10)
WRITE(6,101)NE
101 FORMAT(10I)NUMBER OF ELEMENTS=*,I2)
102 WRITE(6,103)MT
FORMAT(10I)NUMBER OF NODES PER ELEMENT INCLUDING CENTER NODES=*
112) WRITE(6,105)NNODT
105 FORMAT(10I)NUMBER OF TOTAL SYSTEM NODES INCLUDING CENTER NODES=*
1,12)
N=MT-1
106 WRITE(6,106)M
FORMAT(10I)NUMBER OF NODES PER ELEMENT EXCLUDING CENTER NODES=*,I2)
NNODE=NNODT-NE
WRITE(6,107)NNOD
FORMAT(10I)NUMBER OF SYSTEM NODES EXCLUDING CENTER NODES=*,I2)

C C X AND Y COORDINATES FOR MAIN EIGHT NODES
C DO 113 I=1,NNODT
X(I)=0.D0
113 Y(I)=0.D0
WRITE(6,120)MAIN NODE NO.,6X,'X COORD',6X,'Y COORD')
120 FORMAT(10I,M)
DO 112 I=1,M
READ(5,121)K,XM(K),YM(K)
121 FORMAT(12I2F10.5)
112 WRITE(6,122)K,XM(K),YM(K)
122 FORMAT(5X,I2,11X,F10.5,3X,F10.5)
C C ARRAY OF NODE NUMBERS AND FORMATION OF X AND Y COORDINATES.
C C

```



```

170 READ(5,170)NXDIV,NYDIV
170 FORMAT(2I5)
171 WRITE(6,171)NXDIV
171 FORMAT(6,171)NUMBER OF ELEMENT DIVISIONS IN X DIRECTION=*,I3)
172 WRITE(6,172)NYDIV
172 FORMAT(6,172)NUMBER OF ELEMENT DIVISIONS IN THE Y DIRECTION=*,I3)

C CALL NODE(NXDIV,NYDIV)
C CALL XYFORM(NXDIV,NYDIV)

C NUMBER OF NODES LOCATED ON THE NONREFLECTION BOUNDARY
C AND THEIR RESPECTIVE NODE NUMBERS

C READ(5,114)NRBN,X11,X12,ETA1,ETA2
C READ(5,114)NRBN,X11,X12,ETA1,ETA2
114 WRITE(6,131)NRBN
131 FORMAT(6,131)NUMBER OF NODES ON NONREFLECTION BOUNDARY=*,I2)
115 WRITE(6,115)X11,X12
115 FORMAT(6,115)NONREFLECTION BOUNDARY ALONG TOP OF ELEMENT IS FROM
115 1X1=F5*2,1X,*TO X11,F5*2)
116 WRITE(6,116)ETA1,ETA2
116 FORMAT(6,116)NONREFLECTION BOUNDARY ALONG RIGHT SIDE OF ELEMENT IS
116 1FROM ETA=*,F5*2,1X,*TO ETA=*,F5*2)
117 XINC=1.0/NXDIV
117 DO/NXDIV
118 NA=2*NXDIV*NYDIV+NXDIV+NYDIV+1
118 NB=NYDIV*(2*NXDIV+1)
119 NC=NXDIV
119 DO 10 I=1,NRBN
120 IF(X11.EQ.*X12) GO TO 118
120 EN=NA-NB+NC*X11
121 X11=X11+X1INCR
121 IF(X11.LT.X12.OR.X11.EQ.*X12) GO TO 20
121 EN=NA-NB*ETA1+NC
121 ETA1=ETA1-YINCR
20 II=EN
20 NDAMP(II)=NOW(II)
20 CONTINUE
10 WRITE(6,132)
132 FORMAT(6,132)NODE NUMBERS LOCATED ON THE NONREFLECTION BOUNDARY*)
133 FORMAT(5X,I3)
133 FORMAT(5X,I3)(NDAMP(I),I=1,NRBN)

C SPEED OF SOUND AND FLUID DENSITY
C
102 READ(5,102)SOUND,FLDEN
102 FORMAT(2F10.5)
102 WRITE(6,126)SOUND

```



```

126 FORMAT('0','SPEED OF SOUND =',F10.5)
141 FORMAT('6',141)FLDEN
      FORMAT('0',DENSITY OF FLUID=',F10.5)
C C NUMBER OF FLUID NODES AND GLOBAL NODES NUMBERS WHICH
FORCING MECHANISM IS IN CONTACT.
C
148 READ(5,148)NP,ETA1,ETA2
      FORMAT(12,8X,F10.5)
      WRITE(6,149)NP
      FORMAT(6,149)NP
      WRITE(6,152)NP,NUMBER OF NODES IN CONTACT WITH PISTON=':I4'
      WRITE(6,152)ETA1,ETA2
      FORMAT(6,152)RANGE ON LEFT BOUNDARY WHICH PISTON IS IN CONTACT IS F
      151 FORMAT(6,151)NP,TO ETA=',F5.2)
      WRITE(6,151)NP,NODE NUMBERS IN CONTACT WITH FORCING FUNCTION')
      DO 30 I=1,NP
      EN=NA-NB*ETA1-NC
      ETA1=ETA1-YINC
      I1=EN
      NPN(I)=NOW(I)
      WRITE(6,153)NPN(I)
      30 FORMAT(5X,I3)
      153 FORMAT(5X,I3)
C AMPLITUDE OF THE FORCING FUNCTION AT THE INTERFACE NODES')
C WITH WHICH THE FORCING MECHANISM IS IN CONTACT.
C
138 WRITE(6,138)AMPLITUDE OF PISTON AT THE INTERFACE NODES')
      FORMAT(6,139)
      WRITE(6,139)
139 FORMAT('0',4X,'NODE',5X,'AMPLITUDE')
      READ(5,134){AMP(I),I=1,NP}
      FORMAT(9F8.4)
      WRITE(6,137){NPN(I),AMP(I),I=1,NP}
      137 FORMAT(6X,I2,2X,F16.8)
C INITIAL VALUE OF OMEGA IN THE PISTON FORCING FUNCTION, AND TOTAL NUMBER OF OMEGAS FOR
C OMEGA FOR SUCCEEDING SOLUTIONS, AND INCREMENT VALUE OF OMEGA FOR VALUE
C WHICH PROBLEM IS TO BE CALCULATED
C
160 READ(5,160)OMEGA,OINCR,NO
      FORMAT(12F10.5,I2)
      WRITE(6,161)OMEGA
      161 FORMAT('0',161)OMEGA
      WRITE(6,162)OINCR
      162 FORMAT('0',162)INCREMENT VALUE OF OMEGA=',F10.5)
      WRITE(6,163)NO
      163 FORMAT('0',163)NUMBER OF INCREMENTS OF OMEGA=',I2)

```


RETURN
END

SUBROUTINE HQFORM

C IMPLICIT COMPLEX*16 (D),REAL*8 (A-C,E-H,O-Z)
REAL*8 ITITLE
COMMON H(81,81),Q(81,81),B(81)
COMMON RD(50),RDS(50),RDSS(50),X(81),Y(81),HE(8,8),QE(8,8)
COMMON GA(4),GH(4),SF(8),YD(8),YM(8),AMP(25)
COMMON SOUND,FLDEN,OMEGA,UNICR
COMMON NN(100,8),NDAMP(50),NPN(50),NSF(8),NG(8),NN9(50,9),NOW(100)
COMMON NE,M,NNJD,NRBN,NP,ND,NNOD,NC

C SETTING ALL ELEMENTS OF Q AND H EQUAL TO ZERO
DO 20 I=1,NNOD
DO 20 J=1,NNOD
Q(I,J)=0. DO 20 H(I,J)=0. DO

C GAUSS QUADRATURE ABSCISSA VALUES AND WEIGHT COEFFICIENTS
GA(1)= .861136311594053D0
GA(2)= .339981043584856D0
GA(3)= -.339981043584856D0
GA(4)= -.861136311594053D0
GH(1)= .347854845137454D0
GH(2)= .652145154862546D0
GH(3)= -.652145154362546D0
GH(4)= .347854845137454D0

C FORMULATION OF THE ELEMENT HE AND QE MATRICES USING THE 4 TERM GAUSS
QUADRATURE NUMERICAL INTEGRATION SCHEME
DO 21 L=1,NE
DO 22 I=1,M
DO 22 J=1,M
QE(I,J)=0. DO 22 HE(I,J)=0. DO
22
C DO 23 LA=1,4
DO 23 LB=1,4
GX=GA(LA)
GY=GA(LB)
SF(1)= .25D0*(1.0D0-GX)*(1.0D0-GY)*(-GX-GY-i.DG)


```

SF(2) = 5000*(1°DO-GX**2)*(1°DO+GY)*(1°DO-GY-1°DO)
SF(3) = 2500*(1°DO+GX)*(1°DO-GY**2)
SF(4) = 5000*(1°DO+GX)*(1°DO+GY)*(1°DO+GY-1°DO)
SF(5) = 2500*(1°DO+GX**2)*(1°DO+GY)*(1°DO+GY-1°DO)
SF(6) = 5000*(1°DO-GX)*(1°DO+GY)*(1°DO+GY-1°DO)
SF(7) = 2500*(1°DO-GX)*(1°DO-GY**2)
SF(8) = 5000*(1°DO-GX)*(1°DO-GY)*(2°DO*GX+GY)
SF(9) = 2500*(1°DO-GY)*(2°DO*GX-GY)
SF(10)= 5000*(1°DO-GY**2)
SF(11)= 2500*(1°DO+GY)*(2°DO*GX+GY)
SF(12)= -1°DO*(1°DO+GY)*(GX)
SF(13)= 2500*(1°DO-GY)*(2°DO*GX-GY)
SF(14)= 5000*(1°DO-GY**2)
SF(15)= 2500*(1°DO+GY)*(2°DO*GX+GY)
SF(16)= -1°DO*(1°DO+GY)*(GX)
SF(17)= 2500*(1°DO-GY)*(2°DO*GX-GY)
SF(18)= -1°DO*(1°DO+GX)*(2°DO*GY+GX)
SF(19)= 2500*(1°DO+GX)*(2°DO*GY-GX)
SF(20)= -1°DO*(1°DO+GX)*(GY)
SF(21)= 2500*(1°DO+GX)*(2°DO*GY+GX)
SF(22)= -1°DO*(1°DO+GX**2)
SF(23)= 5000*(1°DO-GX)*(2°DO*GY-GX)
SF(24)= 2500*(1°DO-GX)*(GY)
SF(25)= -1°DO*(1°DO-GX)*(GY)
SF(26)= 24 J=0 DO
AJ(1,1)=AJ(1,1)+XD(I,I)*X(NN(L,I))
AJ(1,2)=AJ(1,2)+XD(I,I)*Y(NN(L,I))
AJ(2,1)=AJ(2,1)+YD(I,I)*X(NN(L,I))
AJ(2,2)=AJ(2,2)+YD(I,I)*Y(NN(L,I))
AJDET=AJ(1,1)*AJ(2,2)-AJ(1,2)*AJ(2,1)
AJDET=AJ(1,1)*AJ(2,2)/ADET
AJDET=AJ(1,2)=AJ(2,1)/ADET
AJDET=AJ(2,2)=TEMP/ADET
DO 28 I=1 M
XXD(I)=AJ(1,1)*XD(I,I)+AJ(1,2)*YD(I,I)
YYD(I)=AJ(2,1)*XD(I,I)+AJ(2,2)*YD(I,I)
DO 29 I=1 M
YY=Y+SF(I)*Y(NN(L,I))
COEFH=ADEFH*GH(LA)*GH(LB)*YY
COEFQ=COEFH/SOUND**2
DO 23 LC=1 M
DO 23 LDE=1 M
FUNH=COEFH*(XXD(LC)*XXD(LC)+YYD(LC)*YYD(LC))

```



```

23      FUNQ=COEFF*SF(LC)*SF(LD) + FUNQ
      QE(LC,LD) = QE(LC,LD) + FUNQ
      HE(LC,LD) = HE(LC,LD) + FUNH
      C      ADDING ELEMENT HE AND QE MATRICES TO TOTAL FLUID MATRICES
      C
      25      DO 21 I=1,M
              DO 21 J=1,M
                  II=NN(L,I)
                  JJ=NN(L,J)
                  Q(I,I,J,J)=Q(I,I,J,J)+QE(I,J)
                  H(I,I,J,J)=H(I,I,J,J)+HE(I,J)
              21      RETURN
          END

          SUBROUTINE FDAMP
          IMPLICIT COMPLEX*16 (D),REAL*8 (A-C,E-H,O-Z)
          REAL*8 ITITLE
          COMMON/ITITLE/DSUM(81,81),DB(81)
          COMMON/H(81,81),Q(81,81),B(81),X(81),Y(81),HE(8,8),QE(8,8)
          COMMON/RD(50),RDS(50),ROSS(50),XM(8),YM(8),AMP(25)
          COMMON/GA(4),GH(4),SF(8),XD(8),YYD(8),AJ(2,2),BL(3,3)
          COMMON/FLDEN,OMECA,OINCR
          COMMON/NNDMP(50),NPN(50),NSF(8),NG(8),NN9(50,9),NOW(100)
          COMMON/NE,X,NNGD,NRBN,NP,NO,NNODT,NC
          C      SETTING ELEMENTS OF DAMPING VECTOR EQUAL TO ZERO
          DO 40 I=1,NRBN
              RD(I)=0.0
              RDS(I)=0.0
              RDSS(I)=0.0
          40      RDSS(I)=0.0

          C      FORMULATION OF THE VECTORS RD,RDS,AND RDSS BY THE 4 POINT GAUSS
          C      QUADRATURE NUMERICAL INTEGRATION SCHEME. VECTOR RD REPRESENTS
          C      ELEMENTS ON THE MAIN DIAGONAL, VECTOR RDS REPRESENTS THE FIRST OFF
          C      DIAGONAL ELEMENTS, AND VECTOR RDSS REPRESENTS THE SECOND OFF
          C      DIAGONAL ELEMENTS
          DO 42 K=J-1,NRBN,2
              I=J-2
              II=NDAMP(I)
              JJ=NDAMP(J)
              KK=NDAMP(K)
              DO 42 L=I,4
                  GX=GA(L)

```



```

SF(1) = 5.0DO*(1.0DO-GX)*(-GX)
SF(2) = 1.0DO*(1.0DO-GX)**2
SF(3) = 5.0DO*(1.0DO+GX)
XD(1) = -2.0DO*GX
XD(2) = +2.50DO*GX
XD(3) = +1.0*Y((1.0DO-GX)*(-GX))
YDIF = XD(1)*Y((1.0DO-GX)*(-GX))
SDIF = DSQR(XDIF*XDIF+YDIF*YDIF)
YY=SF(1)*Y((1.0DO-GX)*(-GX))
COEF=YY*SOUND
RD(I)=RD(I)+COEF*SF(1)*SOUND
RD(K)=RD(K)+COEF*SF(2)*SOUND
RD(J)=RD(J)+COEF*SF(3)*SOUND
RDS(1)=RDS(1)+COEF*SF(1)*SF(2)
RDS(2)=RDS(2)+COEF*SF(2)*SF(3)
RDS(3)=RDS(3)+COEF*SF(1)*SF(3)
42 RDS(1)=RDS(1)+COEF*SF(3)

```

42 ADDING SPHERICAL CONTRIBUTION TO THE MATRIX H

```

R=Y(1)
DO 44 I=1,NRBN
II=NDAMP(I)
S=RDS(I)*SOUND/R
H(I,I)=H(I,I)+S
44 DO I=2,NRBN
J=I-1
JJ=NDAMP(J)
II=NDAMP(I)
S=RDS(I)*SOUND/R
H(J,J)=H(J,J)+S
H(I,J)=H(I,J)+S
DO I=3,NRBN,2
J=I-2
JJ=NDAMP(J)
II=NDAMP(I)
S=RDS(I)*SOUND/R
H(J,J)=H(J,J)+S
H(I,J)=H(I,J)+S
48 RETURN
END

```

C C C

SUBROUTINE FORCE

```

C IMPLICIT COMPLEX*16 (D),REAL*8 (A-C,E-H,O-Z)
REAL*8 ITITLE
COMMON DSUM(81,81),DB(81)

```



```

COMMON H(81,81),Q(81,81),B(81),Y(81),X(81),HE(8,8),QE(8,8)
COMMON RD(50),RDS(50),SF(8),YD(8),Y(8),YM(8),AMP(25)
COMMON GA(4),GH(4),X(8),XD(8),XXD(8),YYD(8),AJ(2,2),BL(3,3)
COMMON SOUND,FLDEN,OINCR,NP(50),NPN(50),NSF(8),NG(8),NN9(50,9),NOW(100)
COMMON NN(100,8),NDAMP(50),NP(50),NOD,NNOD,NC
COMMON NE,M,NNOD,NRBN,NP,NO,NNODT,NC

C      SETTING ALL ELEMENTS OF THE PISTON FORCING FUNCTION EQUAL TO ZERO
C
DO 50 I=1,NNOD
  B(I)=0.D0
C      FORMULATION OF THE FORCING FUNCTION USING THE 4 POINT
C      GAUSS QUADRATURE NUMERICAL INTEGRATION SCHEME
C
DO 52 J=3,NP,2
  DO 51 LC=1,3
    DO 51 LD=1,3
      BL(LC,LD)=0.D0
  51 K=J-1
  I=J-2
  II=NPN(I)
  KK=NPN(K)
  JJ=NPN(J)
  ED=DSQRT((Y(II)-Y(JJ))*#2 + (X(II)-X(JJ))*#2)
  DO 54 L=1,4
    GX=GA(L)
    SF(1)= 5.0D0*(1.0D0+GX)*#2
    SF(2)= 1.5D0*(1.0D0-GX)*#2
    SF(3)= 1.5D0*(1.0D0-GX)*(-GX)
    YY=SF(1)*Y(II)+SF(2)*Y(KK)+SF(3)*Y(JJ)
    COEF=(ED/2.0D0)*YY*GH(L)
  DO 54 LA=1,3
    DO 54 LB=1,3
      BL(LA,LB)=BL(LA,LB)+COEF*SF(LA)*SF(LB)
      B(I,I)=B(I,I)+BL(1,1)*AMP(1,2)*AMP(K)+BL(1,3)*AMP(J)
      B(KK)=B(KK)+BL(2,1)*AMP(2,2)*AMP(K)+BL(2,3)*AMP(J)
    52 B(JJ)=B(JJ)+BL(3,1)*AMP(1)+BL(3,2)*AMP(K)+BL(3,3)*AMP(J)
    DO 56 I=1,NP
      II=NPN(I)
    56 B(II)=B(II)*FLDEN
  RETURN
END

```



```

C SUBROUTINE PROB
C IMPLICIT COMPLEX*16 (D),REAL*8 (A-C,E-H,O-Z)
REAL*8 ITITLE
COMMON/ITITLE/DSUM(81,81),DB(81)
COMMON/H(81,81),Q(81,81),X(81),Y(81),HE(8,8),QE(8,8)
COMMON/RD(50),RDS(50),RDSS(50),AMP(25)
COMMON/GA(4),GH(4),SF(8),XD(8),YM(8),XXD(8),YYD(8),AJ(2,2),BL(3,3)
COMMON/SOUND,FLDEN,OMEGA,GINCRC
COMMON/N(100,8),NDAMP(50),NPN(50),NSF(8),NG(8),NN9(50,9),NOW(100)
COMMON/NE,M,NNOD,NRBN,NO,NNODT,NC
DIMENSION/ABPRES(100),PHASE(100)

C INTRODUCING INITIAL VALUE OF OMEGA AND SUBSEQUENT VALUES

DO 70 KOUNT=1,NO
WRITE(6,600) OMEGA
FORMAT(1,"VALUE OF OMEGA FOR THIS RUN=",F10.5)

C SETTING VALUES OF DSUM EQUAL TO ZERO
DO 60 I=1,NNOD
DO 60 J=1,NNOD
DSUM(I,J)=0.0D0,O.D0)

C SUMMING ALL PROBLEM COMPONENTS
DO 62 I=1,NNOD
DO 62 J=1,NNOD
DSUM(I,J)=DSUM(I,J)+H(I,J)-((OMEGA**2)*Q(I,J))
62 DO 63 I=1,NRBN
I=NDAMP(I)
63 DSUM(I,I)=DSUM(I,I)+DCMPLX(0.D0,(OMEGA*RD(I)))
DO 64 J=2,NRBN
I=J-1
I=NDAMP(I)
JJ=NDAMP(J)
DSUM(I,J)=DSUM(I,J)+DCMPLX(0.D0,(OMEGA*RDS(I)))
64 DSUM(J,I)=DSUM(J,I)+DCMPLX(0.D0,(OMEGA*RDS(I)))
DO 65 J=3,NRBN,2
I=J-2
I=NDAMP(I)
JJ=NDAMP(J)
DSUM(I,J)=DSUM(I,J)+DCMPLX(0.D0,(OMEGA*RDS(I)))
65 DSUM(J,I)=DSUM(J,I)+DCMPLX(0.D0,(OMEGA*RDS(I)))

C MULTIPLICATION OF THE FORCING FUNCTION VECTOR B BY OMEGA SQUARED
C AND STORING IN COMPLEX VECTOR D

```



```

C      DO 66  I=1,NNOD
C      DB(I) = DCMLX(B(I)*(OMEGA**2),0.0D0)
66    CONTINUE

C      SOLVING PROBLEM USING SUBROUTINE CSIMEQ
C
C      CALL CSIMEQ (DSUM,DB,NNOD)
C      WRITE(6,610)
C      FORMAT(6,610,'ABSOLUTE VALUE AND PHASE ANGLE OF PRESSURE')
610    WRITE(6,611)
C      FORMAT(6,611,'PRESSURE ON TOP-PHASE ANGLE ON BOTTOM')
611    DO 72 I=1,NNODT
C      ABPRES(I)=0.0D0
72    PHASE(I)=0.0D0
K=0
DO 68 I=1,NNODT
DO 69 J=1,NE
J=NN9(J,9)
IF(JJ.EQ.I) GO TO 68
69  CONTINUE
K=K+1
ABPRES(I)=CDABS(DB(K))
A=DB(K)
AA=DB(K)*(0.0D0,-1.0D0)
PHASE(I)= 57.2957795131D0 * DATAN2(AA,A)
68  CONTINUE
I=1
J=9
615  WRITE(6,612)(ABPRES(K),K=I,J)
612  FORMAT(//9{5X,F9.5})
613  WRITE(6,613)(PHASE(K),K=I,J)
I=I+9
J=J+9
IF(J.LT.82) GO TO 615

C      ACOUSTIC IMPEDANCE AND ENERGY BALANCE

C      WRITE(6,801)
C      FORMAT(6,801,'ACOUSTIC IMPEDANCE')
801  Z=0.0D0
DO 80 J=1,NP
JJ=NPN(J)
Z=Z+B(J)*((DB(JJ)*(0.0D0,-1.0D0))
80  ZZ=ZZ+B(JJ)*DB(JJ)
ZREAL=-2.0D0*3.1415926536D0*Z/(OMEGA*FLDEN)

```



```

ZIMAG=2.0*D0*3.1415926536D0*ZZ/(OMEGA*FLDEN)
TENGO=Z*OMEGA/(2.0*D0*FLDEN)
WRITE(6,803)ZREAL
803 FORMAT(6.0,5X,1REAL=:,F16.8)
FORMAT(6.0,5X,1IMAG=:,F16.8)
804 WRITE(6,814)
FORMAT(6.0,5X,1PROBLEM ENERGY BALANCE:)
814 WRITE(6.0,810)TENGO
810 FORMAT(6.0,5X,1AVG POWER IN=:,F16.8)
DO 84 I=1,NRBN
I=NDAMP(I)
ENGO=ENG0+CDABS(DB(II))*RD(I)*CDABS(DB(II))
84 DO 86 I=2,NRBN
J=I-1
JJ=NDAMP(J)
I=NDAMP(I)
ENGO=ENG0+CDABS(DB(II))*RD(J)*CDABS(DB(JJ))*2.0
DO 88 I=3,NRBN,2
J=I-2
JJ=NDAMP(J)
I=NDAMP(I)
ENGO=ENG0+CDABS(DB(II))*RDSS(J)*CDABS(DB(JJ))*2.0
DO 88 TENGO=ENG0/(2.0*D0*SOUND*FLDEN)
FORMAT(6.812)TENGO
812 FORMAT(6.0,5X,1AVG POWER OUT=:,F15.8)
OMEGA = OMEGA + OINCR
770 RETURN
END

```

```

SUBROUTINE NODE(NXDIV,NYDIV)
C
IMPLICIT COMPLEX*16 (D),REAL*8 (A-C,E-H,O-Z)
REAL*8 ITITLE
COMMON DSUM(81,81),DB(81)
COMMON H(81,81),Q(81,81),X(81),Y(81),HE(8,8),QE(8,8)
COMMON RD(50),RDS(50),RDSS(50),XM(8),YM(8),AMP(25)
COMMON GA(4),GH(4),SF(8),XD(8),YYD(8),AJ(2,2),BL(3,3)
COMMON SOUND,FLDEN,OMEGA,OINCR
COMMON NN(100,8),NDAMP(50),NPN(50),NSF(8),NG(8),NN9(50,9),NOW(100)
COMMON NE,M,NNOD,NRBN,NP,NOD,NC

```

```

ASSIGNING NODE NUMBERS TO ELEMENTS
      WRITE(6,126)
      C
      C
      C

```



```

126 FORMAT('O', 'ASSIGNMENT OF NODE NUMBERS TO ELEMENTS')
      I1=1
      I2=NXDIV
      L=4*NXDIV+3
      K=2*NXDIV+2
      J=1   32  KK=1,NYDIV
      DO 30  I=11,I2
      NN9(I,1)=L
      NN9(I,2)=L+1
      NN9(I,3)=L+2
      NN9(I,4)=K+2
      NN9(I,5)=J+2
      NN9(I,6)=J+1
      NN9(I,7)=J
      NN9(I,8)=K
      NN9(I,9)=K+1
      L=L+2
      K=J+2
      J=J+2*NXDIV+2
      J=J+2*NXDIV+2
      K=K+2*NXDIV+2
      K=K+2*NXDIV
      K1=I2+NXDIV
      32  WRITE(6,127) ELEMENT NO.,5X,'NODE NUMBERS (8 NODDED ELEMENTS)'
      127 FORMAT(6,127)
      DO 31 I=1,NNODT
      NOW(I)=0
      31  I=0
      DO 40 I=1,NNODT
      DO 42 J=1,NE
      JJ=NN9(J,9)
      IF(JJ.EQ.I) GO TO 40
      42  CONTINUE
      I=I+1
      NOW(I)=I
      40  CONTINUE
      DO 34 I=1,NE
      DO 35 J=1,M
      I=NN9(I,J)
      NN(I,J)=NCW(I,I)
      35  WRITE(6,128) NN(I,J), J=1,M
      34  FORMAT(6,128)
      128 FORMAT(3X,I2,11X,8I5)
      RETURN
      END

```


SUBROUTINE XYFORM(NXDIV,NYDIV)

```

C IMPLICIT COMPLEX*16 (D),REAL*8 ( A-C, E-H, O-Z )
C
      REAL*8 ITITLE /
      REAL*8 LABEL/8H
      COMMON H(81,81),Q(81,81),B(81),DB(81),HE(8,8),QE(8,8)
      COMMON RD(50),RDS(50),RDSS(50),XM(8),YN(8),AMP(25)
      COMMON GA(4),GH(4),SF(8),XD(8),YD(8),XXD(8),YYD(8),AJ(2,2),BL(3,3)
      COMMON SOUND,FLDEN,SOMEGR,OINCR
      COMMON NN(100,8),NDAMP(50),NPN(50),NSF(8),NG(8),NN9(50,9),NOW(100)
      COMMON NEWM,NNOD,NR6N,NP,NO,NNODT,NC
      REAL*4 XDRAW,TITLE(12)
      DIMENSION XVAL(25),YVAL(25),XDRAW(25),YDRAW(25),XF(100),YF(100)

      C CALCULATE X AND Y COORDINATES
      C
      XINCR=1.00/NXDIV
      YINCR=1.00/NYDIV
      NX=2*NXDIV+1
      NY=2*NYDIV+1
      DO 10 I=1,NX
      10 XVAL(I)=0.0
      DO 11 I=1,NY
      11 YVAL(I)=0.0
      DO 12 I=2,NX
      12 XVAL(I)=XVAL(J)+XINCR
      YVAL(I)=YVAL(J)-YINCR
      DO 13 I=2,NY
      13 J=I-1
      YVAL(I)=YVAL(J)-YINCR
      14 WRITE(6,121)
      121 FORMAT(6,121)
      11 BE CALCULATED.)
      WRITE(6,126)
      126 FORMAT(6,125)'VALUES OF XI',5X,'VALUES OF ETA')
      125 FORMAT(6,125)'XVAL(I)',11X,'YVAL(I)',I=1,NX)
      LL=1
      DO 16 I=1,NY
      16 DO 17 J=1,NX
      17 GX=XVAL(J)
      GY=YVAL(J)
      SF(1)=.25D0*(1.00-GX)*(1.00-GY)*(-GX-GY-I*DO)

```



```

SF(2)= 500DO*(1.0-GX**2)*(1.0-DO-GY)
SF(3)= *25DO*(1.0+GX)*(1.0-DO-GY)*(+GX-GY-1.0)
SF(4)= *500DO*(1.0+GX)*(1.0-DO-GY)**2
SF(5)= *25DO*(1.0+GX)*(1.0-DO+GY)*(+GX+GY-1.0)
SF(6)= *500DO*(1.0-GX**2)*(1.0+DO+GY)
SF(7)= *25DO*(1.0-DO-GX)*(1.0+DO+GY)*(+GX+GY-1.0)
SF(8)= *500DO*(1.0-DO-GX)*(1.0+DO-GY)*(+GX+GY-1.0)
SF(9)= *25DO*(1.0-DO-GX)*(1.0+DO-GY)**2

DO 28 K=1,M
XF(LL)=XF(LL)+SF(K)*XM(K)
YF(LL)=YF(LL)+SF(K)*YM(K)
DO 27 LL=LL+1
CONTINUE
28 WRITE(6,127) VALUES OF X AND Y'
127 FORMAT(6,128)
128 FORMAT(6,129)
129 FORMAT(6,130)
130 FORMAT(6,131), (X COORDINATES ON TOP-Y COORDINATES ON BOTTOM)
131 I=1*NXDIV+1
J=2*NXDIV+1
N=12*NXDIV+1*(2*NYDIV+1)
132 WRITE(6,133)(L,I,L=I,J)
133 FORMAT(6,134)(X,I,J)
134 FORMAT(6,135)(Y,I,J)
135 FORMAT(6,136)(F8.5)
136 FORMAT(6,137)(F8.5)
137 FORMAT(6,138)(F8.5)
138 FORMAT(6,139)(F8.5)
139 I=I+(2*NXDIV+1)
J=J+(2*NXDIV+1)
140 IF(J.LT.(N+1)) GO TO 124
PLOT CORNER NODES AS 124 POINTS ON A GRAPH

141 I=1
J=2*NXDIV+1
142 J=1*(2*NXDIV+1)*(2*NYDIV)+1
143 NNX=NXDIV+1
NNY=NYDIV+1
KK=4*NXDIV+2
144 LL=1
145 L=I,J=2
146 XDRAW(LL)=XF(L)
YDRAW(LL)=YF(L)
147 LL=LL+1
148
149 DO 15 L=I,J=2
150 XDRAW(LL)=XF(L)
YDRAW(LL)=YF(L)
151
152 K=2
153 IF(I.EQ.1) K=1
154 CALL DRAW(NNX,NDIV+1)
155 I=1*(4*NXDIV+2)

```



```

J=J+(4*NXDIV+2)
IF(J.LT.(N+1)) GO TO 129
18 LL=1 7 L=I I J J K K
DO 17 XDRAW(LL)=XF(L)
YDRAW(LL)=YF(L)
LL=LL+1

K=2 IF(JJ.EQ.N) K=3
CALL DRAW(NNY,XDRAW,YDRAW,K,O,LABEL,ITITLE,0,0,0,0,0,5,7,0, LAST)
I=I+2
JJ=JJ+2
IF(JJ.LT.(N+1)) GO TO 18
DO 34 I=34 I=1,NNOD
X(I)=0 DO 30 I=1,NNODT
Y(I)=0 DO 32 I=1,NE
DO 32 I=32 I=1,NNODT
DD=NN9(J,9)
IF(JJ.EQ.I) GO TO 30
32 CONTINUE
DD=NN9(I,9)
IF(I.I)=XF(I)
Y(I.I)=YF(I)
30 CONTINUE
END

C SUBROUTINE CSIMEQ (A,B,N)
C CSIMEQ IS A SUBROUTINE TO SOLVE EITHER A REAL OR COMPLEX SYSTEM
C OF SIMULTANEOUS EQUATIONS IN WHICH MATRIX A IS ANY SQUARE MATRIX
C AND B IS THE COLUMN VECTOR OF CONSTANTS ON THE RIGHT SIDE OF THE
C EQUATIONS. N IS THE NUMBER OF EQUATIONS IN THE SYSTEM
C
C COMPLEX*16 A(81,81),B(81)
C
DO 401 I=1,N
I1=I+1
B(I)=B(I)/A(I,I)
IF(I-N)402,403,402
402 DO 404 J=1,N
IF(CDABS(A(I,J)).EQ.0.D0) GO TO 404
A(I,J)=A(I,J)/A(I,I)
DO 406 K=J,N
A(K,J)=A(K,J)-A(K,I)*A(I,J)

```

CSIMEQ IS A SUBROUTINE TO SOLVE EITHER A REAL OR COMPLEX SYSTEM
 OF SIMULTANEOUS EQUATIONS IN WHICH MATRIX A IS ANY SQUARE MATRIX
 AND B IS THE COLUMN VECTOR OF CONSTANTS ON THE RIGHT SIDE OF THE
 EQUATIONS. N IS THE NUMBER OF EQUATIONS IN THE SYSTEM

C


```
406 A(J,K)=A(K,J)
404 B(J)=B(J)-A(J,I)*B(I)
401 CONTINUE
C C BACK SUBSTITUTION
403 I1=I
I=I-1
IF(I) 411,411,412
412 DO 413 J=I,N
413 B(I)=B(I)-A(I,J)*B(J)
414 GO TO 403
411 RETURN
END
```


APPENDIX C

ISO-PARAMETRIC ELEMENTS

The family of iso-parametric elements, recently developed by Zienkiewicz, Irons, and others, has brought new versatility and power to the finite element method. The special usefulness of these elements is that they may be shaped to conform to curvilinear boundaries. Attention is confined here to two-dimensional parabolic elements. A full description of the entire family is given in Ref. [2].

Consider the rectangular element of Figure 5. The element has four corner nodes and four midside nodes, numbered as shown. Points in the interior, or on the boundary, may be located in the local (ξ, η) coordinate system. The dependent variable, pressure p in the present application, is defined at any point by Eq. (3), repeated here

$$p = \sum_{i=1}^8 N_i p_i \quad (3)$$

where

$$N_i = \frac{1}{4}(1 + \eta \eta_i)(1 + \xi \xi_i)(\eta \eta_i + \xi \xi_i - 1)$$

for corner node i , and

$$N_i = \frac{1}{2}(1 - \eta^2 \xi_i^2 - \xi^2 \eta_i^2)(1 + \eta \eta_i + \xi \xi_i)$$

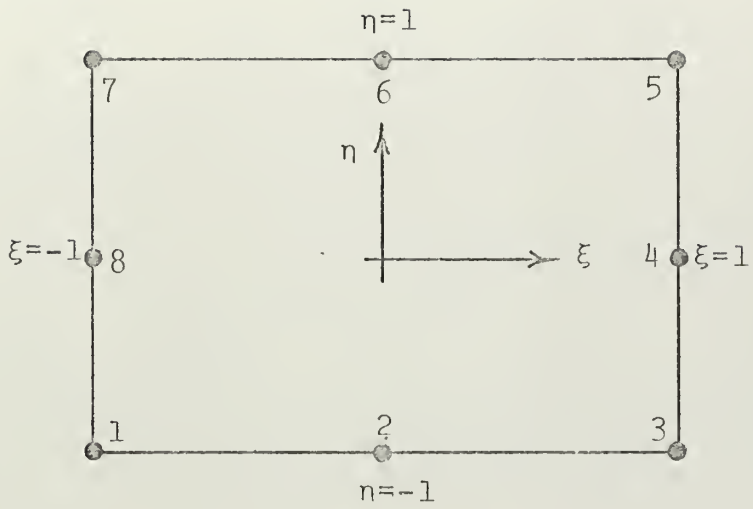


Figure 5. Element Configuration in Local ξ, η Coordinates

for mid-side node i ,

(ξ_i, η_i) are coordinates of node i ,

and p_i is the pressure at node i .

Note that each shape function N_i has the value unity at node i , and is zero at all other nodes.

A curvilinear element, such as that of Figure 6, may be produced by mapping the rectangle of Figure 5 into the x, y plane by the relations

$$x = \sum_{i=1}^8 N_i x_i, \quad y = \sum_{i=1}^8 N_i y_i \quad (19)$$

where (x_i, y_i) are the cartesian coordinates of node i .

The shape of the element in the x, y plane is uniquely determined by specifying the coordinates (x_i, y_i) for the

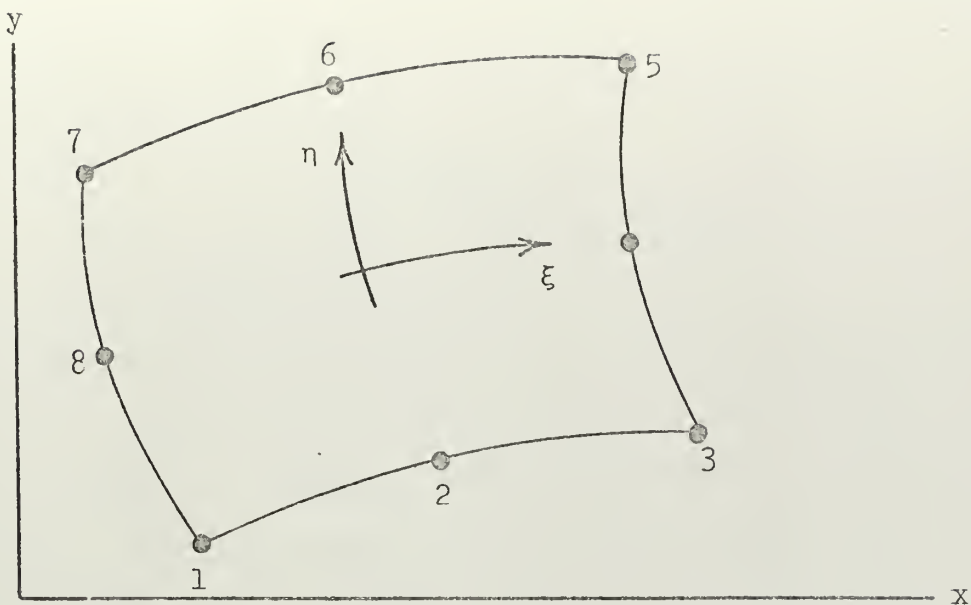


Figure 6. Curvilinear Elements Mapped in Cartesian Coordinates.

eight nodes. The edges of this curvilinear element are parabolic.

Adjacent elements "share" the same three nodes at their interface. When mapped to cartesian coordinates, these two adjacent elements then have the same curvilinear shape and the same x and y coordinates at nodes. This provides continuity in the pressure distribution across element boundaries.

The region developed for the present study necessitates the use of iso-parametric elements to provide the circular non-reflection boundary. This boundary is constructed using parabolic arc segments which are mapped by use of the shape functions to "fit" a quarter circle boundary in cartesian coordinates.

APPENDIX D
FINITE ELEMENT MESH GENERATOR

Two subroutines, included in the computer program of Appendix B, should prove useful in a variety of finite element problems. Together, these subroutines subdivide the region, systematically assign element numbers and node numbers, calculate nodal coordinates, and produce a computer plot of the region to be studied. As an example, consider the region of Figure 7.

The region is taken to be one large iso-parametric element (a mapping of the rectangle of Figure 5). Its shape is prescribed by specifying the (x,y) coordinates of the

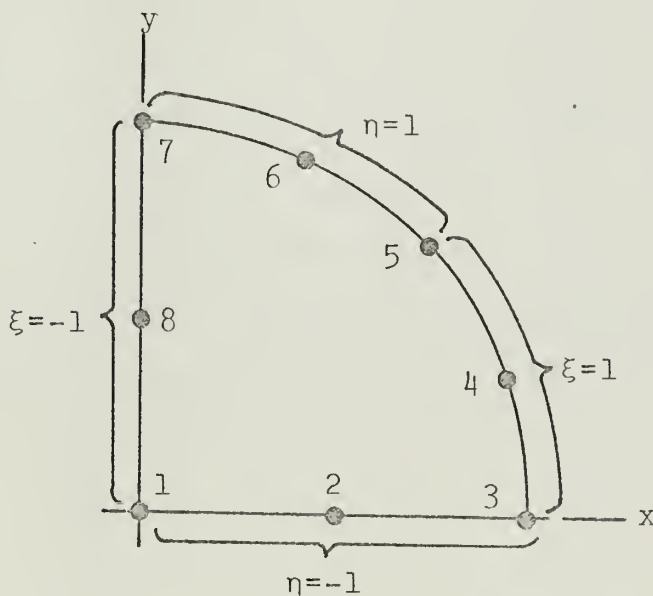


Figure 7. Basic Geometry of Finite Element Region.

eight nodes. Subdivision of the element can then be accomplished at predetermined values of ξ and η by using Equation (19).

Subroutine NODE (Appendix B) requires two input parameters, the number of divisions desired in the x direction and the number of divisions desired in the y direction. These parameters are used to calculate the increment values of ξ and η for subdividing the element into smaller elements. The subroutine starts numbering global nodes at the upper left hand corner ($\xi=-1$, $\eta=1$) then adds increment values of ξ and assigns global node numbers from left to right on the boundary $\eta=1$. Similarly, after incrementing η , the second row of global node numbers is assigned, etc. Global node numbers are assigned to all corner nodes, mid-side nodes and the center of each subdivided element (9 nodes per element). The center node provides unique identification for the element and simplifies the printing of computer output in a readable form. Subsequently all nodes are renumbered, omitting the center nodes.

The cartesian coordinates corresponding to the global node numbers are calculated by a similar process in the subroutine XYFORM and are used in the program to plot the finite element grid. Figure 8 illustrates a computer plot of the finite element mesh generated for a quarter circular region (Figure 7) with an eight foot radius. The number of subdivisions in both the x and y direction is equal to four. The plotting routine produces straight segments

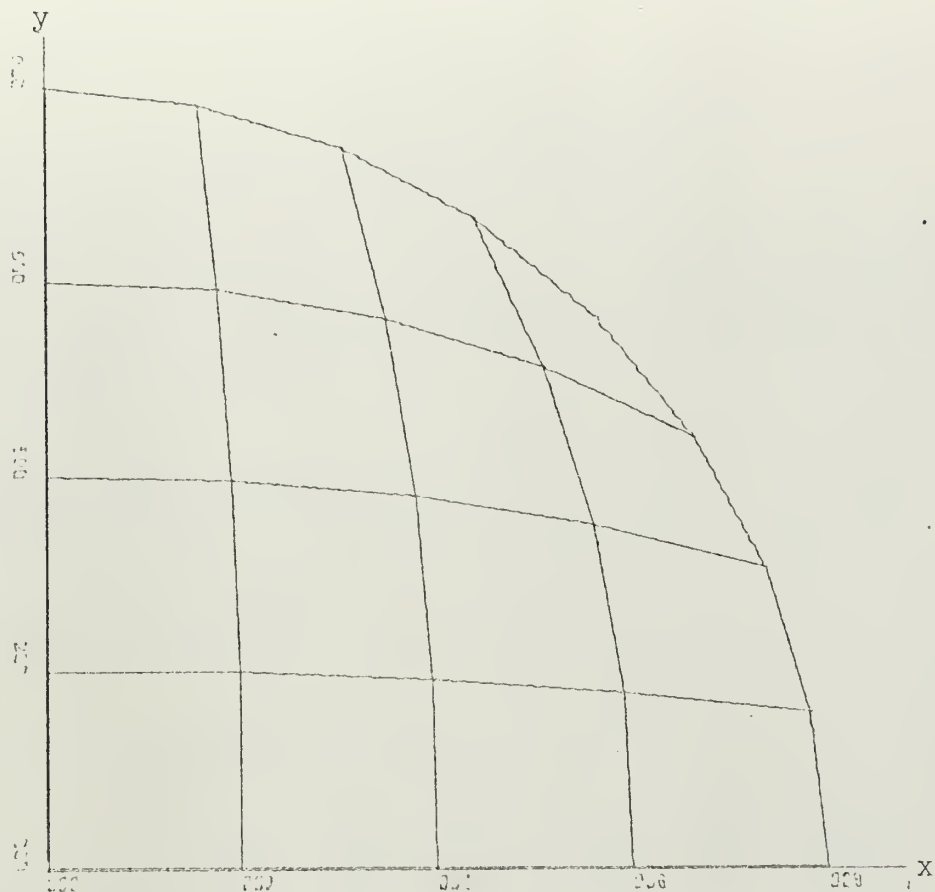


Figure 8. Finite Element Mesh Generated
by Subroutine XYFORM.

between nodes. In this instance, the element boundaries are all parabolic arcs except for those lying on the x and y axes.

APPENDIX E
MATRIX ELEMENT FORMULAS

Individual elements of the matrices $[Q]$, $[D]$, $[L]$, and $[H]$ of the system of ordinary differential equations (Eq. (4)) are given by Ref. [3] as

$$q_{ij} = \frac{1}{c^2} \int_{Re} N_i N_j dR$$

$$d_{ij} = \frac{1}{c} \int_{Se} N_i N_j dS$$

$$\ell_{ij} = \int_{Se} N'_i N'_j dS$$

$$h_{ij} = \iint_{Re} \left[\frac{\partial N_i}{\partial x} \cdot \frac{\partial N_j}{\partial x} + \frac{\partial N_i}{\partial y} \cdot \frac{\partial N_j}{\partial y} + \frac{\partial N_i}{\partial z} \cdot \frac{\partial N_j}{\partial z} \right] dR$$

where Re and Se are the element region and external boundary respectively.

The shape functions N_i , N'_i are specified in terms of local coordinates and it is advantageous to perform the integrations in these coordinates. Gaussian quadrature is employed. Details of the procedure are given in Ref. [2].

LIST OF REFERENCES

1. Hunter, Joseph L., Acoustics, Prentice-Hall, 1957.
2. Zienkiewicz, O. C., Irons, B. M., et al., "Iso-Parametric and Associated Element Families for Two-and Three-Dimensional Analysis," Chapter 13 in Finite Element Methods in Stress Analysis, Holand, I. and Bell, K. (eds.), pp. 403-416, Tapir, Trondhjem, 1969.
3. Zienkiewicz, O. C. and Newton, R. E., "Coupled Vibrations of a Structure in a Compressible Fluid," Proceedings of the Symposium on Finite Element Techniques. University of Stuttgart, Germany, June 1969.
4. Kinsler, L. E., and Frey, A. R., Fundamentals of Acoustics, 2nd ed., John Wiley & Sons, 1962.

INITIAL DISTRIBUTION LIST

No. Copies

1.	Defense Documentation Center Cameron Station Alexandria, Virginia 22314	2
2.	Library, Code 0212 Naval Postgraduate School Monterey, California 93940	2
3.	Professor R. E. Newton Department of Mechanical Engineering Naval Postgraduate School Monterey, California 93940	3
4.	LCDR Dennis V. Dean 1304 Arden Avenue Clearwater, Florida 33515	1
5.	Assoc. Professor G. Cantin Department of Mechanical Engineering Naval Postgraduate School Monterey, California 93940	1
6.	Naval Ship Systems Command Washington, D. C. 20360	1
7.	Professor T. Sarpkaya, Code 59S1 Chairman, Department of Mechanical Engineering Naval Postgraduate School Monterey, California 93940	2

UNCLASSIFIED

Security Classification

DOCUMENT CONTROL DATA - R & D

(Security classification of title, body of abstract and indexing annotation must be entered when the overall report is classified)

1. ORIGINATING ACTIVITY (Corporate author) Naval Postgraduate School Monterey, California 93940		2a. REPORT SECURITY CLASSIFICATION Unclassified
2b. GROUP		
3. REPORT TITLE Finite Element Study of Acoustic Waves		
4. DESCRIPTIVE NOTES (Type of report and inclusive dates) Master's Thesis; December 1970		
5. AUTHOR(S) (First name, middle initial, last name) Dennis Vale Dean, Lieutenant Commander, United States Navy		
6. REPORT DATE December 1970	7a. TOTAL NO. OF PAGES 71	7b. NO. OF REFS 4
8a. CONTRACT OR GRANT NO.	9a. ORIGINATOR'S REPORT NUMBER(S)	
b. PROJECT NO.		
c.	9b. OTHER REPORT NO(S) (Any other numbers that may be assigned this report)	
d.		
10. DISTRIBUTION STATEMENT This document has been approved for public release and sale; its distribution is unlimited.		
11. SUPPLEMENTARY NOTES	12. SPONSORING MILITARY ACTIVITY Naval Postgraduate School Monterey, California 93940	
13. ABSTRACT		

The generation and propagation of small amplitude acoustic waves in a homogeneous, loss-free, compressible fluid is studied by the finite element method. A diaphragm mounted in an infinite rigid baffle generates acoustic waves in a semi-infinite fluid region. Steady-state pressure distribution is found for a hemispherical region with boundary reflection suppressed through use of a radiation condition. The computer program developed for the purpose utilizes iso-parametric finite elements with curvilinear boundaries. Incorporated in the program is a versatile mesh generator which minimizes the quantity of input data. Acceptable agreement with analytic results is obtained when there are at least four elements per wave-length.

UNCLASSIFIED
Security Classification

KEY WORDS	LINK A		LINK B		LINK C	
	ROLE	WT	ROLE	WT	ROLE	WT
FINITE ELEMENTS						
ACOUSTIC WAVES						
RADIATION IMPEDANCE						

DD FORM 1 NOV 65 1473 (BACK)
S/N 0101-807-6821

Thesis 124370
D1828 Dean
c.1 Finite element study
of acoustic waves.

10 SEP 71 18485
31 JUL 82 812923+1
25 JAN 90 13806

Thesis 124370
D1828 Dean
c.1 Finite element study
of acoustic waves.

thesD1828
Finite element study of acoustic waves.



3 2768 002 10073 7

DUDLEY KNOX LIBRARY